Isonimesulide and Its Carborane Analogues as Isoform-Selective COX Inhibitors and Antitumor Agents

Liridona Useini, Teodora Komazec, Markus Laube, Peter Lönnecke, Jonas Schädlich, Sanja Mijatović, Danijela Maksimović-Ivanić, Jens Pietzsch, and Evamarie Hey-Hawkins*

Nonsteroidal anti-inflammatory drugs (NSAIDs) are the most widely used therapeutics against pain, fever, and inflammation; additionally, antitumor properties are reported. NSAIDs reduce the synthesis of prostaglandins by inhibiting the cyclooxygenase (COX) isoforms COX-1 and COX-2. As nonselective inhibition is associated with off-target effects, strategies to achieve selectivity for the clinically preferred isoform COX-2 are of high interest. The modification of NSAIDs using carborane clusters as phenyl mimetics is reported to alter the selectivity profile through size exclusion. Inspired by these findings, isonimesulide and its carborane derivatives are prepared. The biological screening shows that the carborane containing compounds exhibit a stronger antitumor potential compared to nimesulide and isonimesulide. Furthermore, the replacement of the phenyl ring of isonimesulide with a carborane moiety resulted in a shift of the COX activity from nonactive to COX-active compounds.

L. Useini, P. Lönnecke, E. Hey-Hawkins
Faculty of Chemistry and Mineralogy
Institute of Inorganic Chemistry
Leipzig University
04103 Leipzig, Germany
E-mail: hey@uni-leipzig.de

T. Komazec, S. Mijatović, D. Maksimović-Ivanić
Department of Immunology
Institute for Biological Research "Siniša Stanković"
National Institute of the Republic of Serbia
University of Belgrade
11060 Belgrade, Serbia

M. Laube, J. Schädlich, J. Pietzsch
Department of Radiopharmaceutical and Chemical Biology
Institute of Radiopharmaceutical Cancer Research
Helmholtz-Zentrum Dresden Rossendorf (HZDR)
01328 Dresden, Germany

J. Pietzsch
Faculty of Chemistry and Food Chemistry
School of Science
Technical University Dresden
01069 Dresden, Germany

1. Introduction

Nimesulide or *N*-(4-nitro-2-phenoxyphenyl)methanesulfonamide is a nonsteroidal anti-inflammatory drug (NSAID) with potent anti-inflammatory, analgesic, and antipyretic properties.[1,2] It is used for treatment of acute pain, arthritic conditions, musculoskeletal problems, headaches, fever, cancer pain, and vascular diseases.[3,4] Due to its COX-2 selectivity and other mechanisms that nimesulide is involved in (e.g., inhibition of leucocyte respiratory burst through inhibition of phosphodiesterase type IV, inhibition of superoxide anion and hypochlorous acid formation in activated neutrophils, prevention of oxidative and proteolytic inactivation of the α_1-proteinase inhibitor, as well as reduction of the extracellular availability of hypochlorous acid),[5–7] there is a growing interest for its application in cancer therapy.[3,8–11] Furthermore, it is used as an alternative therapeutic for NSAID-intolerant patients that suffer from allergic reactions like NSAID-induced asthma.[7,12] An oral administration of nimesulide twice per day (100–200 mg) proved to be more effective than other conventional NSAIDs (indomethacin, ibuprofen, and naproxen),[2,6,13] causing milder adverse effects on the gastrointestinal tract, due to its COX-2 selectivity.[14] However, prolonged usage of nimesulide induces hepatic failure; thus, its therapy is limited to a maximum of 15 days.[15,16]

Nimesulide was discovered in 1971 by George Moore and collaborators and was licensed for production in 1985.[5,8] It was first introduced to markets in Italy and Portugal; nowadays it is available in more than 50 countries worldwide.[6,8] Due to its hepatotoxicity and other safety issues, nimesulide was withdrawn from the market in Finland and Spain in 2002 and in Ireland in 2007; it was never approved for distribution in the USA, UK, Canada, and New Zealand.[8]

Considering the hepatotoxicity associated with nimesulide usage[15,17] and the aim to improve its selective anti-inflammatory and anticancer activity, research has focused on developing nimesulide-based derivatives with higher potency, improved selectivity, better pharmacological profile, and fewer side effects. Due to its application as an alternative therapeutic for NSAID-intolerant patients[12] and its potential in cancer treatment, nimesulide was used as an inspiration to design new drugs; therefore, many nimesulide-based compounds have been reported in the past.[8,18–20]

**ADVANCED
SCIENCE NEWS**

www.advancedsciencenews.com
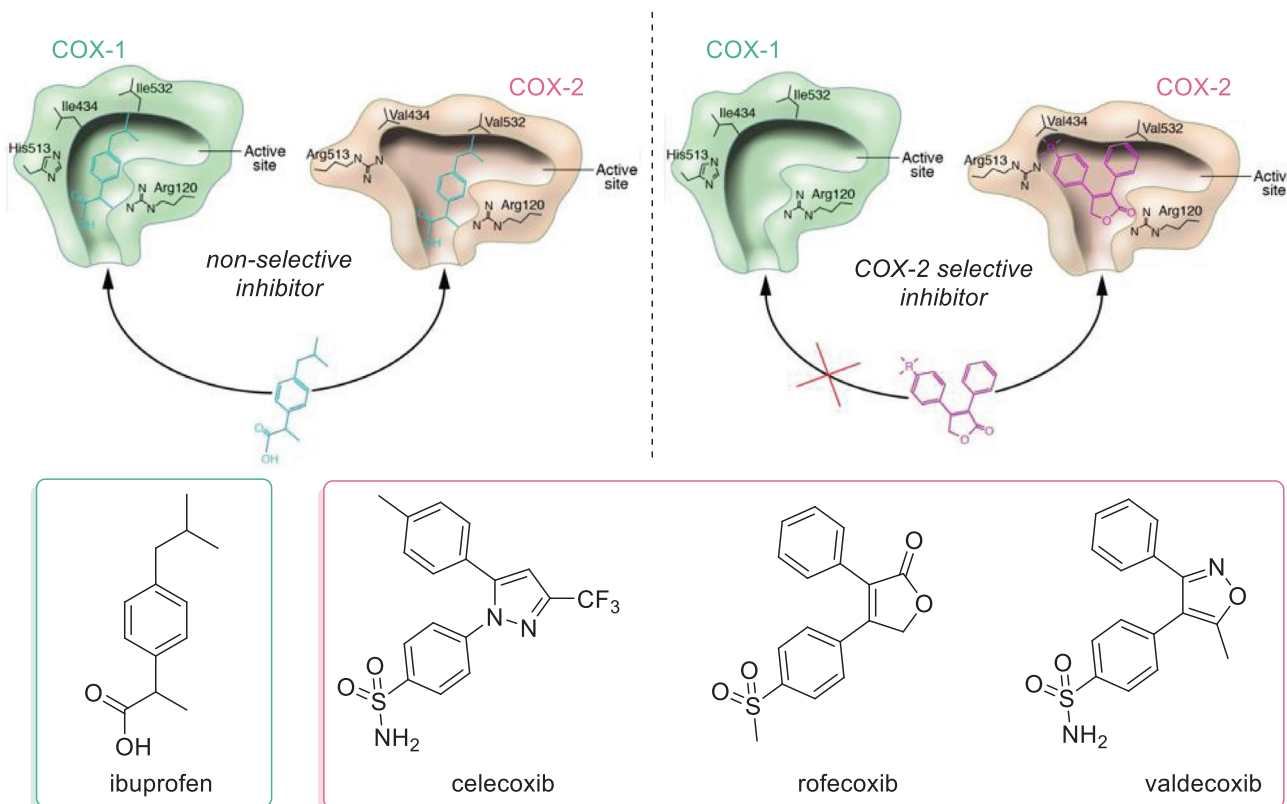
**ADVANCED
THERAPEUTICS**

www.advtherap.com

Figure 1. The difference in mode of action between a conventional NSAID (left) and COX-2 selective NSAID (right). Nonselective COX-inhibitor (ibuprofen) and the COXIBs (celecoxib, rofecoxib, and valdecoxib). Reproduced with permission.[30] Copyright 2006, American Society for Clinical Investigation.

Like other NSAIDs, nimesulide blocks cyclooxygenase, the homodimer proteins located in the membrane of the endoplasmic reticulum,[21] with reported IC$_{50}$ values of 10.48 μM (COX-1) and 0.18 μM (COX-2).[22] Therefore, it reduces the transformation of arachidonic acid to prostaglandins (PGs), which are the mediators of many signaling pathways including, among others, pain, fever, and inflammation.[23] Research on morphology[24] and mode of action[25] have focused on the two main COX isoforms: COX-1, which is found in most of the tissues where it moderates the homeostatic processes, and COX-2, also known as the "induced isoform" because it is closely related with nonphysiological processes, such as pain, fever, and inflammation.[26] Beside their differences in the mode of action,[27,28] COX isoforms share a high identity in peptide sequence; thus, many conventional NSAIDs nonselectively bind to both isoforms (**Figure 1**).[29]

In order to maintain the homeostasis and the overall wellbeing, the balance between proinflammatory and physiologic prostaglandin production must be well moderated. Thus, the metabolic process of COX-1 should not be influenced, while the production of proinflammatory PGs should be blocked.[31] This would ideally be achieved by a COX-2 selective inhibitor.[32] Due to an accessible side pocket (Figure 1), the active site of the COX-2 isoform is ≈25% larger than that of the COX-1;[33] therefore, a size enlargement of the drug could yield the desired selectivity.[34] This hypothesis was confirmed, when cele-

coxib, rofecoxib, and valdecoxib (Figure 1) were introduced to the market.[35] The bulkier molecules, compared to ibuprofen, showed highly selective activity toward COX-2 and regardless of their plasma concentration they never inhibited COX-1.[35,36]

The interest toward NSAIDs was further advanced, when their anticancer properties were discovered.[37] Epidemiologic studies report that patients who were exposed to NSAIDs showed lower prevalence for cancer diseases. Furthermore, a continuous usage of NSAIDs resulted in prevention of carcinogenesis which led to the proposal to use NSAIDs as an early stage cancer treatment.[38,39] This mode of action can be explained by the fact that some cancer cells manifest an overexpression of the COX-2 isoform; thus, the proinflammatory prostaglandins are produced inducing further the proinflammatory genes.[39,40] Therefore, the inhibition of COX-2 will block this process, and thus, the proliferation of the malignant cells will be blocked or even apoptosis through additional COX-independent off-target mechanisms will be induced.[41] Ferreira et al. reviewed the anticancer properties of nimesulide and the mechanisms that are involved therein. They report that nimesulide increases the levels of PTEN (phosphatase and tensin homolog) expression, and thus inhibits proliferation and causes apoptosis of pancreatic cancer cells.[11] Other in vitro studies report that nimesulide suppresses the growth of hypopharyngeal carcinoma cancer cells via antiproliferation and apoptosis-inducing pathways.[9] Furthermore, nimesulide is reported to inhibit the progression of human ovarian cancer
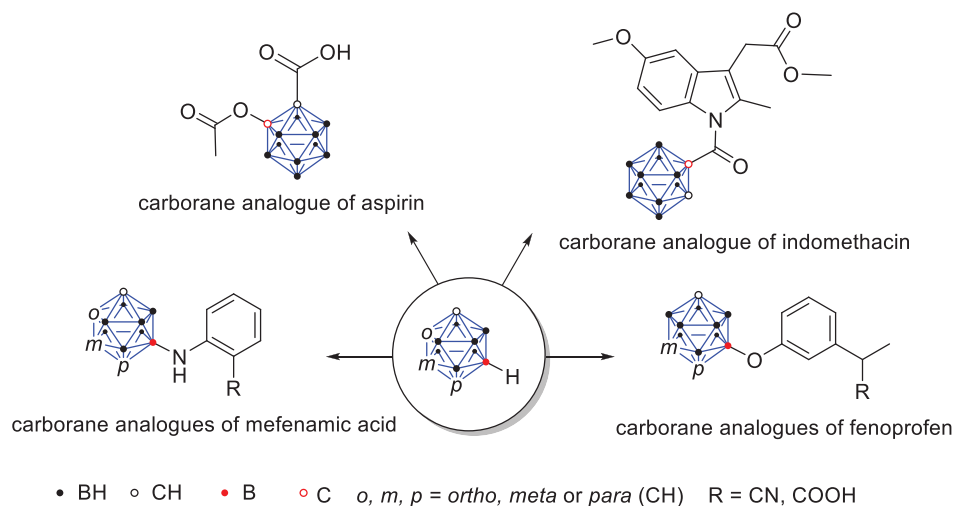
**ADVANCED
SCIENCE NEWS**

www.advancedsciencenews.com

**ADVANCED
THERAPEUTICS**

www.advtherap.com

Figure 2. Carborane analogues of aspirin,[62] indomethacin,[63] mefenamic acid,[64] and fenoprofen.[65]

cells,[42] lung cancer cell proliferation,[5] and induce apoptosis in breast cancer cells.[43]

The above-mentioned reports for NSAIDs and specifically nimesulide motivated both medicinal chemists and pharmaceutical industry to work further on designing drugs with similar properties, or find a way to further modify the commercially available drugs in order to improve their pharmacological profile, like enhancement of COX-isoform selectivity and antitumor potential. A recent strategy is the use of carborane as bioisosteric replacement of the phenyl ring as a hydrophobic moiety.[28,44–51]

Carboranes are boron-based compounds in which at least one BH unit from $closo$-$B_{12}H_{12}^{2-}$ is substituted with a CH vertex.[49,52] From this class, the dicarba-$closo$-dodecaboranes are the compounds of our interest. They are neutral icosahedral clusters with two CH vertices and the general formula $C_2B_{10}H_{12}$.[52,53] Depending on the position of the CH units within the cluster, three different isomers exist: $ortho$-$(1,2$-$C_2B_{10}H_{12})$, $meta$-$(1,7$-$C_2B_{10}H_{12})$, and $para$-carborane $(1,12$-$C_2B_{10}H_{12})$ (**Figure 2** and Scheme 1, compounds **2–4**).[28,46,52,54] Compared to phenyl rings, they are more hydrophobic and exhibit higher metabolic, thermal, and chemical stability. Furthermore, the structural analogy of a rotating phenyl ring with the 3D icosahedral shape of carboranes made carboranes a great tool for structural modification of a wide range of chemicals, especially for drug design in medical chemistry.[28,44,46–48,55–60] Thus, carboranes are used as hydrophobic moieties for structural modification of commercially available drugs,[28,49,57–60] among them many commercial NSAIDs (Figure 2).[51,56,61–65]

The carborane analogue of aspirin (acetylsalicylic acid), asborin, was the first compound to be published,[62] followed by the carborane analogue of indomethacin,[63] and more recently the carborane analogues of mefenamic acid[64] and fenoprofen[65] (Figure 2). For the three last compounds, the carborane analogues showed higher antitumor potential compared to their commercially available organic counterparts. Furthermore, the $nido$-carborane derivative of mefenamic acid and the $meta$-

carborane analogue of fenoprofen bearing a nitrile group were the most potent compounds for COX inhibition. However, no isoform selectivity was observed.[64,65] The aimed COX-2 selectivity shift was so far observed only for the $nido$-carborane analogue of indomethacin, indoborin.[63] These results indicate the existence of potential off-targets mechanisms inside the cells and thus make the carborane analogues of NSAIDs interesting COX-independent antitumor agents.

2. Results and Discussion

2.1. Modifications of the Nimesulide Structure

The nimesulide structure can be modified in different positions (**A–F**, **Figure 3**); several structural modifications of nimesulide were already performed.[8] In order to understand the structure–activity relationship of nimesulide, Catarro et al. reviewed some of the most promising modifications yielding a range of nimesulide-based derivatives.[8] Substitution of the phenyl ring (**A**) with a cyclohexyl moiety[8,66] afforded a compound (NS-389, Figure 3) with improved inhibition potential and higher specificity toward the COX-2 isoform compared to nimesulide. Therefore, the gastrointestinal and renal adverse damage was reduced.[8] Introducing a methyl group at the nitrogen atom (**D**) of NS-398 resulted in loss of COX-2 inhibition potential. The amine proton and the sulfonamide group proved to be very significant for determination of the COX inhibition potential.[67] Changes in position **B** of nimesulide lead to a different biological profile, depending on the specific class of compounds. Nakamura et al. reported that the presence of sulfur and oxygen atoms in position **B** of nimesulide-based derivatives leads to a higher biological activity compared to the nitrogen-bridged derivatives,[68] while in case of pyridine-based nimesulide derivatives (Figure 3), the nitrogen-bridged derivatives were the best anticancer agents with an IC_{50} value of 0.09 μm.[69]
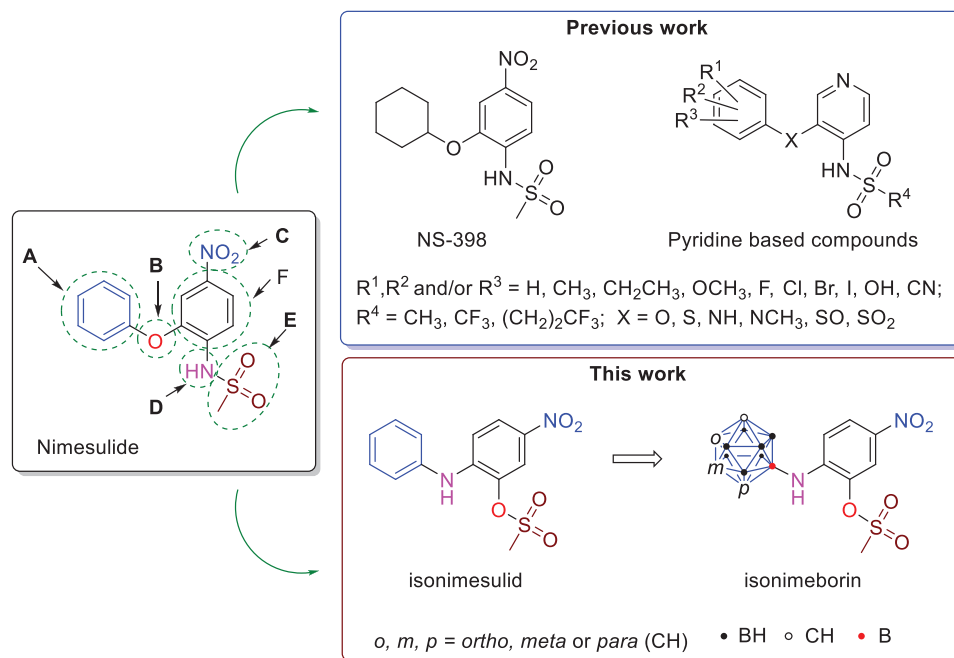
Figure 3. Possible modifications of nimesulide (**A**–**F**), its cyclohexyl (NS-389) and pyridine derivatives,[8] the isomer isonimesulide and its carborane analogues (isonimeborin).
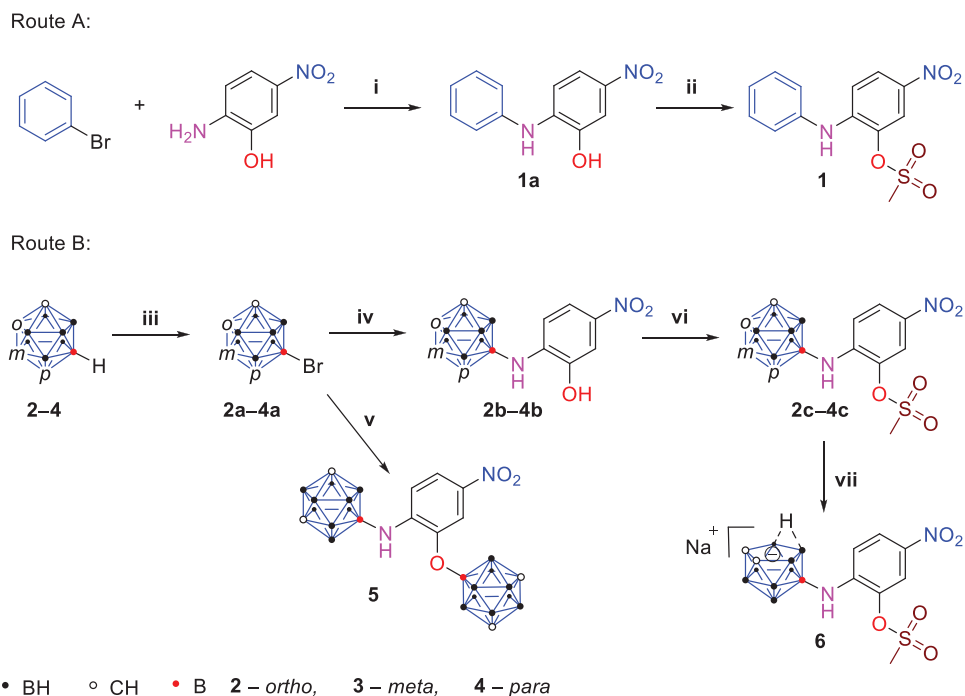
All attempts to prepare the carborane analogues of nimesulide (modification **A**) via a Pd-catalyzed B–O coupling reaction failed (details are given in Tables S8 and S9, Supporting Information). Metal-catalyzed cross-coupling reactions of halogenated carboranes were evaluated[64,65] and reviewed previously,[70–74] showing that Pd-catalyzed B–O coupling of halo-carboranes was a much more challenging task[65,72] compared to B–N coupling reactions.[64,73,74] For such experiments, the use of electron-rich biaryl phosphine ligands is very important.[65,70] Thus, the B–N coupling of halo-carboranes in the synthesis of the carborane analogues of mefenamic acid was successfully accomplished for all the three carborane isomers using either Pd(dba)$_2$–BINAP–KOt-Bu (dba = dibenzylideneacetone; BINAP = 2,2′-bis(diphenylphosphino-1,1′-binaphthyl) or SPhos-Pd-G3–SPhos–K$_3$PO$_4$ (SPhos-Pd-G3 = 2-dicyclohexylphosphino-2′,6′-dimethoxybiphenyl [2-(2′-amino-1,1′-biphenyl)]palladium(II) methanesulfonate; SPhos = 2-dicyclohexylphosphino-2′,6′-dimethoxybiphenyl) as catalyzing system in 1,4-dioxane,[64] while the B–O coupling of halogenated $ortho$-carboranes (9-I-C$_2$B$_{10}$H$_{11}$ and 9-Br-C$_2$B$_{10}$H$_{11}$) with 2-(3-hydroxyphenyl)propionitrile in the synthesis of the carborane analogues of fenoprofen failed.[65] This is due to the low reactivity and the concurrent deboronation of halogenated $ortho$-carboranes under Lewis-basic conditions.[28,50] Correspondingly, we failed to synthesize the oxygen-bridged carborane analogues of nimesulide via a Pd-mediated B–O coupling reaction. These trials and further discussion of the obstacles observed in the B–O coupling attempts are given in Schemes S1 and S2 of the Supporting Information.

Therefore, we have focused on modifications in positions **A**–**D** and in substitution pattern (**F**), while the sulfonyl moiety (**E**) remained unchanged (Figure 3).

2.2. Synthesis of Isonimesulide and Its Carborane Analogues

In order to understand the structure-related properties of nimesulide and evaluate the COX-inhibition profile as well as the cytotoxicity we performed modifications targeting positions **A**–**D**. First, isonimesulide (**1**, **Scheme 1**, route A) was prepared in a two-step synthesis. Bromobenzene was reacted with 2-amino-5-nitrophenol in a Pd-catalyzed Buchwald–Hartwig-type cross-coupling reaction to give 5-nitro-2-(phenylamino)phenol (**1a**), which was mesylated with methanesulfonyl chloride in pyridine to afford the final product **1** in 64% yield. The corresponding carborane derivatives (**2c**–**4c**) (isonimeborin) were synthesized in three steps (Scheme 1, route B) by halogenation of carborane clusters (iii), followed by a Pd-catalyzed B–N cross-coupling reaction (iv), and mesylation of the corresponding carboranyl-amino-nitrophenols (vi). All new compounds were fully characterized.

The halogenation of the three carborane isomers (**2**–**4**) was conducted following published procedures (iii).[64,65] The brominated carborane derivatives (**2a**–**4a**) were then employed in a Pd-catalyzed B–N cross-coupling with 2-amino-5-nitrophenol in 1,4-dioxane and SPhos-Pd-G4–SPhos–KOt-Bu (SPhos-Pd-G4 = 2-dicyclohexylphosphino-2′,6′-dimethoxybiphenyl [2-(N-methylbiphenyl-2′-amine)]palladium(II) methanesulfonate) as catalytic system giving the carboranyl-amino-nitrophenols **2b**–**4b** in moderate to good yields (32–81%) (iv). Additionally, the B–N cross-coupling reaction of 9-Br-1,7-C$_2$B$_{10}$H$_{11}$ (**3a**) and 2-amino-5-nitrophenol in a 1:1 molar ratio afforded the disubstituted compound **5** (36%) only (v). When the reaction was conducted in a 1:2 ratio, **3b** was obtained in 81% yield. Mesylation of **2b**–**4b** was performed in a mixture of pyridine and methanesulfonyl chloride yielding the final products isonimeborin (**2c**–**4c**) in good

**ADVANCED
SCIENCE NEWS**
www.advancedsciencenews.com

**ADVANCED
THERAPEUTICS**
www.advtherap.com

Scheme 1. Synthesis of isonimesulide (**1**) (route A) and its carborane derivatives (**2c–4c**) (route B). Reaction conditions: i) SPhos-Pd-G4, SPhos, KOt-Bu, 1,4-dioxane, 110 °C, 17 h, 6%; ii) MsCl, pyridine, −20 °C to r.t., 18 h, 64%; iii) for **2a** and **3a**: 0.5–1 equiv. Br$_2$, HNO$_3$/H$_2$SO$_4$ (1:1, v/v), AcOH, 60–80 °C, 1 h (83% and 74%), or for **4a**: AlCl$_3$ in CS$_2$, reflux, 21 h (70%);[64,65] iv) 2 equiv. 2-amino-5-nitrophenol, SPhos-Pd-G4, SPhos, KOt-Bu, 1,4-dioxane, 50–70 °C, 20 min to 19.5 h, 32–81%; v) 1 equiv. 2-amino-5-nitrophenol, SPhos-Pd-G4, SPhos, KOt-Bu, 1,4-dioxane, 70 °C, 25 min, 36%; vi) MsCl, pyridine, −20 °C to r.t., 3.5–21 h, 52–95%; and vii) only for **2c**: NaF, EtOH/H$_2$O (3:2, v/v), 90 °C, 3 h, >99%.

yields (vi). *Nido*-isonimeborin **6** was obtained quantitatively by deboronation of **2c** with NaF in EtOH/H$_2$O at 90 °C (vii).

2.3. Biological Evaluation: Potential for COX Inhibition and Cytotoxicity

With isonimesulide (**1**) and the corresponding carborane analogues **2b–4b**, isonimeborins **2c–4c**, disubstituted derivative **5**, and *nido*-isonimeborin **6** in hand we set out to evaluate their potential as COX-isoform inhibitor and anticancer activity. The compounds proved to be stable in dimethyl sulfoxide (DMSO)-d_6 (according to ^{1}H-NMR and ^{11}B{^{1}H}-NMR spectroscopy) for one week (**2b** and **2c**) as compounds started slowly to deboronate, while the other analogues remained stable for more than two months.

2.3.1. COX Inhibition Studies and Hydrophobicity

Nimesulide (**Ref-1**), isonimesulide (**1**), and carborane derivatives (**2b–4b**, **2c–4c**, **5**, and **6**) were tested in vitro for their inhibition potential toward ovine COX-1 and human recombinant COX-2 using the COX Fluorescent Inhibitor Screening Assay Kit (Cayman Chemical Company) and compared with the selective COX-2 inhibitor celecoxib (**7**) as well as the COX-1 inhibitor SC-560 (**8**) as controls (**Table 1**).

An initial screening of compounds at a concentration of 100 μ$\textsc{m}$ revealed that isonimesulide (**1**), a structural isomer of

nimesulide (**Ref-1**), showed no inhibition potential toward both COX isoforms. However, replacement of the phenyl ring in isonimesulide (**1**) by a carborane moiety resulted in COX activity exceeding even the inhibition potential of nimesulide (**Ref-1**). Of note, COX-2 inhibition by nimesulide showed high variance in the concentration range above 10 μ$\textsc{m}$ impeding proper IC$_{50}$ determination (see Figure S76, Supporting Information); however, an IC$_{50}$(COX-2) could be estimated to be in the range of 23 μ$\textsc{m}$ based on all performed experiments.

Of all carborane derivatives, the carboranyl-amino-nitrophenols **2b–4b** as well as *nido*-carborane derivative **6** showed inhibition of cyclooxygenases and were further characterized regarding the COX inhibition profile. The *ortho*-carboranyl-amino-nitrophenol **2b** and the *nido*-carborane derivative **6** resulted to be nonselective inhibitors of both COX isoforms in the low and intermediate micromolar range, respectively (**2b**: IC$_{50}$(COX-1) = 4.4 μ$\textsc{m}$ and IC$_{50}$(COX-2) = 1.9 μ$\textsc{m}$; **6**: IC$_{50}$(COX-1) = 17.5 μ$\textsc{m}$ and IC$_{50}$(COX-2) = 16.9 μ$\textsc{m}$). Interestingly, COX-2 selective inhibition was observed for the *meta-* and *para*-carboranyl-amino-nitrophenols **3b** and **4b** (IC$_{50}$(COX-2) = 2.2 and 1.8 μ$\textsc{m}$, respectively; IC$_{50}$(COX-1) >100 μ$\textsc{m}$) making them a promising scaffold for further tests and structural modifications. Of note, conversion of **2b–4b** to the isonimeborin derivatives **2c–4c** abolished COX inhibition activity (Table 1) although the formed pharmacophore is normally characteristic for this substance class.[19,75]

The lipophilicity of the compounds **1**, **2b–4b**, **2c–4c**, **5**, and **6** was determined as a logD$_{7.4, \text{HPLC}}$ value by an HPLC method originally described by Donovan and Pescatore[76] (Table 1; Table S10,

Table 1. COX inhibition potential of nimesulide (**Ref-1**), isonimesulide (**1**), and carborane derivatives **2b–4b**, **2c–4c**, **5**, and **6**, compared to celecoxib (**7**) and SC-560 (**8**) and their lipophilicity (logD$_{7.4}$).

	% inhibition@ 100 μM[a]		IC$_{50}$ [μM]		SI[b]	logD$_{7.4, HPLC}$
	COX-1	COX-2	COX-1	COX-2		
Ref-1	n.i.	55.3	>100	≈23[c]	>4.3	1.63
1	n.i.	n.i.	n.d.	n.d.	–	4.32
2b	106.4	102.8	4.4	1.9	23	3.76
3b	45.5	84	>100	2.2	>45.5	3.79
4b	30.3	81.8	>100	1.8	>55.6	3.91
2c	17.1	44.5	n.d.	n.d.	–	4.32
3c	n.i.	6.9	n.d.	n.d.	–	4.37
4c	6.8	15.4	n.d.	n.d.	–	4.62
5	9.7	27.1	n.d.	n.d.	–	4.55
6	96.6	93.6	17.5	16.9	1.1	3.49
7[d]	–	–	n.d.	0.089	–	n.d.
8[d]	–	–	0.007	n.d.	–	n.d.

[a] n.i. = no inhibition (% inhibition below 5%) [b] Selectivity index, SI = IC$_{50}$(COX-1)/IC$_{50}$(COX-2) [c] Estimated based on combined data set of four experiments, refer to main text and the Supporting Information for further details. [d] Celecoxib served as reference for COX-2: pIC$_{50}$ (pIC$_{50}$ = −log$_{10}$(IC$_{50}$[M])) was found to be 7.05 ± 0.08; SC-560 served as reference for COX-1: pIC$_{50}$ was found to be 8.12 ± 0.56; for both mean ± SD is given, $n = 3$.

Supporting Information). The logD$_{7.4, HPLC}$ value for nimesulide (**Ref-1**) was determined to be 1.63 and found to be consistent with previous reports.[20] Isonimesulide (**1**) lacking the methyl-sulfonamide group, was found to be considerably more lipophilic (logD = 4.32) in comparison. The isonimeborin analogues **2c–4c** and **5** interestingly showed however a comparable lipophilicity in the range of 4.32–4.62 although the more lipophilic carborane cluster was present. Consistent with the respective chemical transformations, the carboranyl-amino-nitrophenol derivatives **2b–4b** (logD = 3.76–3.91) as well as the *nido* derivative **6** (logD = 3.49) were found to be more hydrophilic compared to the isonimeborin derivatives **2c–4c**.

2.3.2. Studies of the Cytotoxic Potential

The anticancer properties of isonimesulide (**1**) and the carborane derivatives **2b–4b**, **2c–4c**, **5**, and **6** were tested against two human colorectal carcinoma (HT29 and HCT116), hormone-dependent breast adenocarcinoma (MCF-7), human melanoma (A375), and lung carcinoma (A549) cell lines. Cell lines were selected according to their COX-2 expression status. HT29 is COX-2 overexpressing, MCF-7, A549, and A375 are COX-2 positive,[77] while HCT116 is defined as COX-2 negative.[78] Cells were exposed to compounds **Ref-1**, **1**, **2b–4b**, **2c–4c**, **5**, and **6** in a wide range of doses continuously for 72 h, and viability was assessed using 3-(4,5-dimethythiazol-2-yl)-2,5-diphenyltetrazolium bromide (MTT) and crystal violet (CV) tests. While nimesulide (**Ref-1**) did not affect the viability in dose ranges up to 130 μM, isonimesulide (**1**) showed a moderate effect, with IC$_{50}$ values varying from ≈50 to 150 μM (**Table 2**; Figures S77–S79, Supporting Information). On the other hand, the carborane derivatives displayed a heterogeneous potential to limit cancer cell growth in vitro, from completely inactive compound **5** to the most cytotoxic compounds **4b** and **4c**. Therefore, only compounds **4b** and **4c** and isonimesulide (**1**) for comparison were further evaluated.

The IC$_{50}$ values calculated from both tests exhibited a moderate deviation from each other. Since both assays showed deficiencies in the determination of the cell number under certain circumstances, microscopic evaluation was used to select the assay which is more appropriate for calculating the IC$_{50}$ values.[79] Accordingly, IC$_{50}$ values obtained by CV were found as more relevant; therefore, these values were used in further studies of the mechanism of action of **1**, **4b**, and **4c**. The selectivity of these compounds toward malignant phenotype, primary human fibroblast MRC-5, and mouse peritoneal exudate cells PEC was studied under the same experimental conditions. IC$_{50}$ values obtained by CV test revealed that **4b**, and especially **4c**, showed higher selectivity toward neoplastic cells (selectivity index (SI) from 3 to 10 depending on the cell line, **Table 3**).

Furthermore, the basic mechanism behind the antitumor potential of the most potent carborane derivatives **4b** and **4c** was further evaluated on the most sensitive COX-2 positive hormone-dependent MCF-7 cell line. Cells were exposed to the IC$_{50}$ dose of **4b**, **4c** or **1**, and flow cytometric analysis of cell proliferation, presence of cell death, total caspase activity, and production of reactive oxygen and nitrogen species (ROS/RNS) was conducted. Except for the production of ROS/RNS, where the treatment was reduced to 48 h with the aim of more precise determination of oxidative stress, cell divisions as well as death were assessed after 72 h of incubation.

As shown in **Figure 4**A, exposure to the IC$_{50}$ doses of **4b** or **4c** results in a robust mitotic arrest, with an increased contribution of nondividing cells to the total population, compared to the untreated control, and a more profound effect than the reference compound **1**. Annexin V/propidium iodide (PI) double staining revealed that **4b**, but not **4c**, promoted strong apoptosis (Figure 4B) which is not mediated by enhanced caspase activation (Figure S80, Supporting Information). This highlighted mechanistic differences between the carborane-based derivatives of isonimesulide and isonimesulide itself in vitro, as the reference compound **1** triggered caspase-mediated apoptosis and blocked

**ADVANCED
SCIENCE NEWS**

www.advancedsciencenews.com

**ADVANCED
THERAPEUTICS**

www.advtherap.com

Table 2. IC$_{50}$ values [µM] of nimesulide (**Ref-1**), isonimesulide (**1**), and carborane derivatives (**2b–4b**, **2c–4c**, **5**, and **6**) on cancer cell lines. Data are presented as mean ± SD of three independent experiments for MTT and CV tests.

	HCT116		HT29		MCF-7		A375		A549	
	MTT[a]	CV[b]	MTT	CV	MTT	CV	MTT	CV	MTT	CV
Ref-1	170.4 ± 3.2	199.3 ± 1.0	166.2 ± 0.3	194.6 ± 7.7	130.9 ± 12.9	145.5 ± 3.6	141.8 ± 12.5	181.3 ± 9.5	139.0 ± 1.1	197.2 ± 4.0
1	50.5 ± 2.2	74.6 ± 1.6	72.6 ± 6.4	75.9 ± 8.4	67.0 ± 1.3	70.2 ± 2.5	123.8 ± 7.4	108.4 ± 3.0	47.4 ± 3.0	86.3 ± 4.4
2b	15.9 ± 0.2	30.5 ± 3.3	34.9 ± 3.4	45.0 ± 2.6	38.0 ± 2.5	35.7 ± 3.6	45.9 ± 3.0	50.5 ± 5.4	19.0 ± 1.7	37.8 ± 1.4
2c	11.0 ± 0.3	20.7 ± 2.2	12.1 ± 0.3	16.8 ± 1.1	–	–	–	–	–	–
3b	13.0 ± 1.0	29.0 ± 3.0	37.0 ± 0.8	43.7 ± 0.9	10.5 ± 1.4	19.2 ± 1.0	32.0 ± 3.0	38.2 ± 2.2	15.7 ± 1.0	35.0 ± 3.7
3c	14.3 ± 1.4	20.5 ± 0.5	9.0 ± 0.1	11.4 ± 0.1	11.4 ± 1.1	16.1 ± 1.4	–	–	9.6 ± 0.8	18.8 ± 1.8
4b	6.4 ± 0.1	13.8 ± 0.8	32.8 ± 1.6	39.5 ± 3.3	6.1 ± 0.0	9.6 ± 0.1	10.8 ± 0.0	18.0 ± 0.1	8.3 ± 0.2	16.2 ± 0.3
4c	9.5 ± 0.9	19.5 ± 1.4	6.9 ± 0.3	10.9 ± 0.4	6.1 ± 0.7	11.7 ± 0.1	21.0 ± 0.5	21.8 ± 0.9	8.7 ± 0.8	21.7 ± 2.0
5	–	–	–	–	–	–	–	–	–	–
6	79.0 ± 4.3	91.1 ± 1.5	69.9 ± 6.2	71.7 ± 2.1	134.8 ± 3.9	89.6 ± 8.1	135.0 ± 4.5	138.8 ± 7.4	139.6 ± 8.1	131.5 ± 11.8

[a] 3-(4,5-Dimethylthiazol-2-yl)-2,5-diphenyltetrazolium bromide [b] Crystal violet.

Table 3. IC$_{50}$ [µM] values of isonimesulide (**1**) and *para*-carborane derivatives **4b** and **4c** on primary cells. Data are presented as mean ± SD of three independent experiments for CV test.

	PEC	MRC-5
1	85.1	–
4b	23.9	21.3
4c	95.8	84

proliferation at a significantly lower rate than its carborane analogues. Flow cytometric data were supported by fluorescent microscopy of PI stained cell cultures. Dominant apoptosis manifested as irregular shape of nuclei, and enhanced intensity of fluorescence reflecting chromatin condensation was evident upon the treatment with **4b** and reference compound **1** (**Figure 4**C).

Finally, the differences in cellular response to treatment of MCF-7 cells with carborane-based compounds (**4b** and **4c**) and isonimesulide (**1**) were supported with different redox response to the treatment. Thus, while **4b** exerted scavenging potential, **4c** and reference compound **1** did not change the production of hydrogen peroxide and peroxynitrite as measured by dihydrorhodamine 123 (DHR) dye (**Figure 5**A). On the other hand, intracellular production of NO was not affected by any of the tested drugs (Figure 5B). Taken together, the introduction of the carborane cluster into isonimesulide resulted in novel properties, reflected in strong antitumor potential opening numerous possibilities of their potential usage.

3. Conclusion

The nimesulide isomer isonimesulide **1** and its carborane analogues (**2b–4b** and **2c–4c** (isonimeborin)) as well as a biscarborane substituted (**5**) and the *nido*-carborane derivative (**6**) were prepared and fully characterized. While the Pd-catalyzed B–N coupling reaction to give the carborane analogues of isonimesulide was successful, all attempts to prepare the oxygen-

bridged nimesulide analogues failed. In vitro evaluation of COX isoform inhibition potential showed that isonimesulide (**1**) was inactive. However, the carborane derivatives showed even higher COX-inhibition potential than nimesulide. Thus, compounds **2b** and **6** were found to be nonselective, while for compounds **3b** and **4b** COX-2 selective inhibition in lower micromolar range was observed. In vitro cytotoxicity studies showed that isonimesulide (**1**) was a more potent antitumor agent compared to the parent nimesulide. The cytotoxic potential was further enhanced by replacement of the phenyl ring in isonimesulide with a carborane moiety affording compounds **2b–4b** and **2c–4c** (isonimeborin). While compounds **4b** and **4c** were the most potent antitumor agents for the tested cancer cell lines, compound **5** was not active at all. In summary, the structural modification of nimesulide using carboranes as hydrophobic moieties yielded compounds with more potent, but COX-independent antitumor potential; therefore, off-target mechanisms will now be further investigated.

4. Experimental Section

Synthesis: Materials and Methods: All commercially available reagents were purchased from common suppliers and used without further purification. Reactions including carboranes were carried out under a nitrogen atmosphere using the Schlenk technique. For column chromatography, silica gel (60 Å) from Acros was used. The particle size was in the range of 0.035–0.070 mm. Reactions were monitored by thin-layer chromatography (TLC) using silica gel 60 F$_{254}$-coated glass plates from Merck with a fluorescence indicator. Carborane-containing compounds were stained with a 5% solution of palladium dichloride in methanol. 1,4-Dioxane was dried over CaH and further distilled over sodium/benzophenone prior to use and stored over 4 Å molecular sieve under nitrogen.

NMR data were collected with an Avance DRX 400 spectrometer (^{1}H-NMR, 400.13; ^{13}C-NMR, 100.63 MHz; ^{11}B-NMR, 128.38 MHz) or an Ascend 400 spectrometer (^{1}H-NMR, 400.16 MHz; ^{13}C-NMR, 100.63 MHz; ^{11}B-NMR, 128.38 MHz) from Bruker. The ^{1}H- and ^{13}C-NMR spectra were referenced to tetramethylsilane and the ^{11}B-NMR spectra to the Ξ-scale.[80] The numbering scheme is given in the Supporting Information. Deuterated solvents with a deuteration rate of 99.80% were purchased from Eurisotop. The chemical shifts are reported in parts per million (ppm).
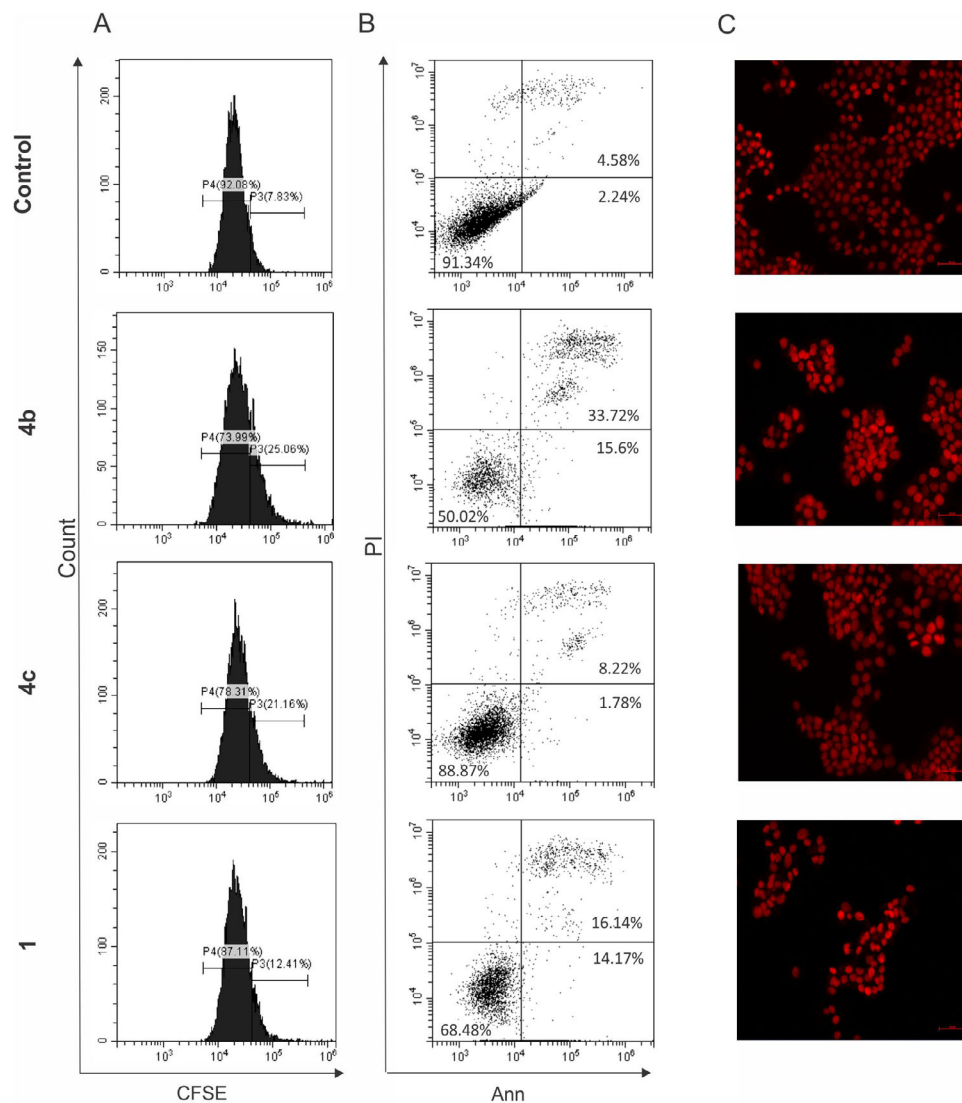
Figure 4. Mode of action of compounds **1**, **4b**, and **4c**. MCF-7 cells were treated with an IC_{50} dose of **1**, **4b**, and **4c** for 72 h and stained with A) carboxyfluorescein diacetate succinimidyl ester (CFSE) and B) Annexin V/PI and analyzed by flow cytometry. One representative experiment out of three is shown. C) Fluorescent microscopy of propidium iodide (PI) stained cells.
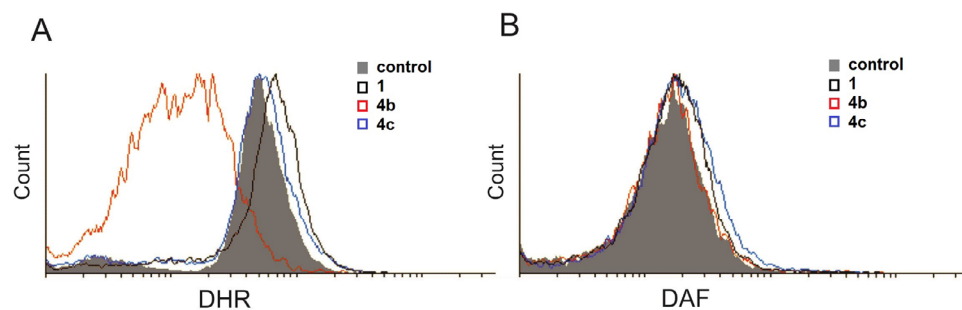

Figure 5. Production of ROS/RNS. MCF-7 cells were treated with an IC_{50} dose of **1**, **4b**, and **4c** for 48 h, stained with A) DHR or B) 4-amino-5-methylamino-2',7-'difluorofluorescein (DAF-FM) diacetate and analyzed by flow cytometry. One representative experiment out of three is shown.

High-resolution ESI mass spectrometry (HR-ESI-MS) was carried out on an Impact II from Bruker Daltonics. The simulation of the mass spectra was conducted with a web-based program from Scientific Instrument Services Inc. (Palmer, MA, USA).[81]

The IR spectra were obtained with a Nicolette IS5 (ATR) from Thermo Fisher Scientific (Waltham, MA, USA). The signal intensity was classified as weak (w), medium (m), or strong (s).

Analysis of purity by Ultra Performance Liquid Chromatography (UPLC) (254 nm): samples were monitored at 254 nm using the following UPLC system: column Aquity UPLC BEH C18 column (waters, 150 × 2.1 mm, 1.7 µm, 130 Å), UPLC (waters, Milford, MA, USA): binary solvent manager UPB, sample manager UPA, column manager UPM, and diode array detector PDA, γ detector Gabi Star (Raytest), flowrate 0.4 mL min^{-1}, eluent (A) 0.1% trifluoroacetic acid in H_2O, (B) MeCN; gradient: $t_{0\ min}$ 95/5 − $t_{0.3\ min}$ 95/5 − $t_{5.3\ min}$ 5/95 − $t_{6.5\ min}$ 5/95 − $t_{6.8\ min}$ 95/5 − $t_{10\ min}$ 95/5.

Data for X-ray structures for compounds **2b–4b**, **2c–4c**, and **5** were collected on a Gemini diffractometer (Rigaku Oxford Diffraction) using Mo-K$_\alpha$ and Cu-K$_\alpha$ radiation (λ = 71.073 pm and 154.184 pm). Data reduction was performed with CrysAlis Pro[82] including the program SCALE3 ABSPACK[83] for empirical absorption correction. All structures were solved by dual-space methods with SHELXT-2018[84] and refined with SHELXL-2018.[85] Further details are given in the Supporting Information. CCDC 2254258 (**2b**), 2254259 (**3b**), 2254260 (**4b**), 2254490 (**2c**), 2254491 (**3c**), 2254492 (**4c**), and 2254261 (**5**) contain the supplementary crystallographic data for this paper. These data can be obtained free of charge from The Cambridge Crystallographic Data Centre via www.ccdc.cam.ac.uk/structures/.

The melting points were determined in glass capillaries using a Gallenkamp apparatus and are uncorrected.

The brominated carborane isomers **2a–4a** were prepared according to previously reported procedures.[54,64,65] The catalysts SPhos-Pd-G3 and SPhos-Pd-G4 were purchased from Sigma-Aldrich or synthesized following the reported protocol (see the Supporting Information for details).[86]

Synthesis of Isonimesulide (5-nitro-2-phenylamino)phenyl methanesulfonate (1): The synthesis of **1a** is given in the Supporting Information.

A 50 mL round-bottom flask was charged with **1a** (36.8 mg; 0.16 mmol) and 1 mL of pyridine. The solution was stirred at −20 °C for 10–15 min. Then 1.1 equiv. of methanesulfonyl chloride (MsCl, 13.6 µL, 0.17 mmol) was added dropwise and the resulting mixture was stirred at room temperature for 3 h. The reaction was stopped by adding 20 mL of ice-cold water. A yellow suspension formed which was transferred to a separatory funnel. The product was extracted with diethyl ether (3 × 20 mL). The combined organic phases were washed with 5 M aqueous HCl (10 mL) and distilled water (10 mL), and dried over MgSO$_4$. Evaporation of the solvent gave the pure product as yellow-brown paste. Yield 64.1% (31.6 mg, 0.1 mmol). TLC (n-hexane/ethyl acetate, 3:2 (v/v)): R$_f$ = 0.47; ^{1}H-NMR ((CD$_3$)$_2$CO): δ 8.25 (d, $^3J_{HH}$ = 2.7 Hz, 1H, CH$_{aryl}$), 8.23 (s, 1H, NH), 8.09 (dd, $^3J_{HH}$ = 9.3, 2.6 Hz, 1H, CH$_{aryl}$), 7.45 (dd, $^3J_{HH}$ = 8.5, 7.3 Hz, 2H, CH$_{aryl}$), 7.41–7.33 (m, 2H, CH$_{aryl}$), 7.30–7.20 (m, 2H, CH$_{aryl}$), 3.50 (s, 3H, CH$_3$) ppm. ^{13}C{^{1}H}-NMR ((CD$_3$)$_2$CO): δ 144.5 (C, C-1), 139.2 (C, C-1'), 138.1 (C, C-5), 135.3 (C, C-2), 129.6 (CH, C-3' and C-5'), 125.2 (CH, C-4'), 124.0 (CH, C-3), 123.5 (CH, C-2' and C-6'), 119.4 (CH, C-4), 112.8 (CH, C-6), 37.3 (C, CH$_3$) ppm. IR (ATR, cm^{-1}): 3373 (m, νNH), 3080 (m-w, νCH), 1590–1494 (m-w, νCC), 1500 (s, νNO$_2$), 1297 (m, νCN), 1153 (m, νSO); HR-ESI-MS (positive mode, MeCN), m/z [M+Na]$^+$: calculated for C$_{13}$H$_{12}$N$_2$O$_5$SNa: 331.0365, found 331.0380; the observed isotopic pattern is in agreement with the calculated one. HPLC: t_R = 5.23 min; purity: 99.7% relative area.

General Procedure for the B–N Cross-Coupling Reaction: An oven dried 50–100 mL Schlenk flask was charged with the corresponding bromocarborane (**2a–4a**), 2-amino-5-nitrophenol, base, catalyst, and ligand, and was evacuated three times and filled with nitrogen. The mixture was then suspended in dry 1,4-dioxane (10 mL). The resulting suspension was placed in a preheated oil bath and stirred for 25 min to 19.5 h at 50–70 °C. The progression of the reaction was followed by TLC (silica gel, n-hexane/ethyl acetate, 4:1, (v/v)). In the end, the reaction mixture was cooled to room temperature and diluted with dichloromethane or diethyl ether. The resulting suspension was filtered through a celite pad. The filtrate was collected and the solvent removed to give the crude prod-

ucts as oils. Further purification via column chromatography (silica gel, n-hexane/ethyl acetate, 1:0–4:1 (v/v)) yielded the pure products as solids. From the pure fractions, single crystals were obtained by liquid layering technique.

2-[N-(1,2-Dicarba-closo-dodecaboran-9-yl)]-5-nitrophenol (2b)

2b was synthesized by reacting **2a** (111.6 mg, 0.5 mmol), 2 equiv. of 2-amino-5-nitrophenol (154.1 mg, 1 mmol), 1.1 mmol of KOt-Bu (121 mg), 5 mol% SPhos-Pd-G4 (19.8 mg), and 5 mol% SPhos (10.2 mg) in dry 1,4-dioxane (10 mL). The mixture was stirred at 50 °C for 19.5 h. Purification via column chromatography over silica gel and mixture of n-hexane/ethyl acetate (3:2, v/v) gave **2b** as orange powder. Yield: 32.1 % (47.5 mg, 0.16 mmol). Single crystals were obtained by layering a saturated Et$_2$O solution of **2b** with n-hexane. Melting point (M.p.) 208–210 °C. TLC (n-hexane/ethyl acetate, 3:2 (v/v)): R$_f$ = 0.45; ^{1}H-NMR ((CD$_3$)$_2$CO): δ 9.27 (s, 1H, OH), 7.72 (dd, $^3J_{HH}$ = 9.0, 2.6 Hz, 1H, CH$_{aryl}$), 7.62 (d, $^3J_{HH}$ = 2.6 Hz, 1H, CH$_{aryl}$), 7.14 (d, $^3J_{HH}$ = 9.0 Hz, 1H, NH), 4.59 (s, 1H, CH$_{cluster}$), 4.56 (s, 1H, CH$_{cluster}$), 2.97–1.86 (br, 9H, BH) ppm. ^{11}B{^{1}H}-NMR ((CD$_3$)$_2$CO): δ 7.4 (s, 1B, BNH), −4.1 (s, 1B, BH), −10.1 (s, 2B, BH), −14.6 (s, 2B, BH), −15.7 (s, 2B, BH), −16.3 (s, 2B, BH) ppm. ^{11}B-NMR ((CD$_3$)$_2$CO): δ 7.4 (s, 1B, BNH), −4.1 (d, J_{BH} = 148.0 Hz, 1B, BH), −10.1 (d, J_{BH} = 149.5 Hz, 2B, BH), −13.9 to −17.0 (br, 6B, BH) ppm. ^{13}C{^{1}H}-NMR ((CD$_3$)$_2$CO): δ 144.8 (C, C-2), 142.2 (C, C-4), 136.9 (C, C-1), 117.9 (CH, C-6), 109.9 (CH, C-5), 108.2 (CH, C-3), 52.3 (CH, C$_{cluster}$), 45.2 (CH, C$_{cluster}$) ppm. IR (ATR, cm^{-1}): 3388 (m, νNH), 3240 (s, νOH), 3080 (m-w, νCH), 2601 (s, νBH), 1593–1464 (m-w, νCC), 1519 (s, νNO$_2$), 1260 (m, νCN), 747 (m, νBB); HR-ESI-MS (positive mode, MeCN), m/z [M+Na]$^+$: calculated for C$_8$H$_{17}$B$_{10}$N$_2$O$_3$: 297.2243, found 297.2250; the observed isotopic pattern is in agreement with the calculated one. HPLC: t_R = 5.44 min; purity: 98.8% relative area.

2-[N-(1,7-Dicarba-closo-dodecaboran-9-yl)]-5-nitrophenol (3b)

3b was synthesized by reacting **3a** (111.6 mg, 0.5 mmol), 2 equiv. of 2-amino-5-nitrophenol (154.1 mg, 1 mmol), 1.1 mmol of KOt-Bu (121 mg), 5 mol% SPhos-Pd-G4 (19.8 mg), and 5 mol% SPhos (10.2 mg) in dry 1,4-dioxane (10 mL). The mixture was stirred at 50 °C for 35 min. Purification via column chromatography (silica gel, n-hexane/ethyl acetate, 7:3 (v/v)) gave **3b** as orange powder. Yield: 81.1 % (120 mg, 0.40 mmol). Single crystals were obtained by layering a saturated CH$_2$Cl$_2$ solution of **3b** with n-hexane. M.p. 237−238 °C. TLC (n-hexane/ethyl acetate, 3:2 (v/v)): R$_f$ = 0.49; ^{1}H-NMR ((CD$_3$)$_2$CO): δ 9.35 (s, 1H, OH), 7.76 (dd, $^3J_{HH}$ = 9.0, 2.6 Hz, 1H, CH$_{aryl}$), 7.65 (d, $^3J_{HH}$ = 2.6 Hz, 1H, CH$_{aryl}$), 7.23 (d, $^3J_{HH}$ = 9.0 Hz, 1H, NH), 5.15 (s, 1H, CH$_{cluster}$), 3.71 (s, 2H, CH$_{cluster}$), 3.20–1.53 (br, 9H, BH) ppm. ^{11}B{^{1}H}-NMR ((CD$_3$)$_2$CO): δ 1.5 (s, 1B, BNH), −7.6 (s, 2B, BH), −11.3 (s, 1B, BH), −14.1 (s, 2B, BH), −15.3 (s, 2B, BH), −18.6 (s, 1B, BH), −22.6 (s, 1B, BH) ppm. ^{11}B-NMR ((CD$_3$)$_2$CO): δ 1.5 (s, 1B, BNH), −7.7 (d, J_{BH} = 162.2 Hz, 2B, BH), −11.4 (d, J_{BH} = 148.8 Hz, 1B, BH), −13.5 to −16.0 (br, 4B, BH), −18.7 (d, J_{BH} = 182.3 Hz, 1B, BH), −22.7 (d, J_{BH} = 184.4 Hz, 1B, BH) ppm. ^{13}C{^{1}H}-NMR ((CD$_3$)$_2$CO): δ 144.9 (C, C-2), 143.5 (C, C-4), 137.2 (C, C-1), 117.9 (CH, C-6), 110.3 (CH, C-5), 108.2 (CH, C-3), 52.3 (CH, C$_{cluster}$) ppm. IR (ATR, cm^{-1}): 3393 (m, νNH), 3241 (s, νOH), 3066 (m-w, νCH), 2595 (s, νBH), 1591–1449 (m-w, νCC), 1519 (s, νNO$_2$), 1290 (m, νCN), 730 (m, νBB); HR-ESI-MS (negative mode, MeCN), m/z [M−H]$^-$: calculated for C$_8$H$_{15}$B$_{10}$N$_2$O$_3$: 295.2086, found 295.2090; the observed isotopic pattern is in agreement with the calculated one. HPLC: t_R = 5.44 min; purity: 98.8% relative area.

2-[N-(1,12-Dicarba-closo-dodecaboran-2-yl)]-5-nitrophenol (4b)

4b was synthesized by reacting **4a** (111.6 mg, 0.5 mmol), 2 equiv. of 2-amino-5-nitrophenol (154.1 mg, 1 mmol), 1.1 mmol of KOt-Bu (121 mg), 5 mol% SPhos-Pd-G4 (19.8 mg), and 5 mol% SPhos (10.2 mg) in dry 1,4-dioxane (10 mL). The mixture was stirred at 50 °C for 20 min. Purification via column chromatography (silica gel, n-hexane/ethyl acetate, 7:3 (v/v)) gave **4b** as an orange powder. Yield: 62.6 % (92.8 mg, 0.31 mmol). Single crystals were obtained by layering a saturated THF solution of **4b** with n-pentane. M.p. 245−246 °C. TLC (n-hexane/ethyl acetate, 7:3 (v/v)): R$_f$ = 0.37; ^{1}H-NMR ((CD$_3$)$_2$CO): δ 9.43 (s, 1H, OH), 7.83 (dd, $^3J_{HH}$ = 9.0, 2.6 Hz, 1H, CH$_{aryl}$), 7.67 (d, $^3J_{HH}$ = 2.7 Hz, 1H, CH$_{aryl}$), 7.46 (d, $^3J_{HH}$ = 9.0 Hz, 1H, CH$_{aryl}$), 5.38 (s, 1H, NH), 3.89 (s, 1H, CH$_{cluster}$), 3.53 (s, 1H, CH$_{cluster}$), 3.03–1.57 (br, 9H, BH) ppm. ^{11}B{^{1}H}-NMR ((CD$_3$)$_2$CO): δ −3.5 (s, 1B, BNH), −14.3 (s, 2B, BH), −15.7 (s, 4B, BH), −16.7 (s, 2B, BH), −20.6

© 2023 The Authors. Advanced Therapeutics published by Wiley-VCH GmbH

**ADVANCED
SCIENCE NEWS**

www.advancedsciencenews.com

**ADVANCED
THERAPEUTICS**

www.advtherap.com

(s, 1B, BH) ppm. ^{11}B-NMR ((CD$_3$)$_2$CO): δ –3.5 (s, 1B, BNH), –13.6 to –17.4 (br, 8B, BH), –20.6 (d, J_{BH} = 167.6 Hz, 1B, BH) ppm. ^{13}C{^{1}H}-NMR ((CD$_3$)$_2$CO): δ 143.9 (C, C-2), 143.8 (C, C-4), 138.2 (C, C-1), 117.6 (CH, C-6), 111.3 (CH, C-5), 108.4 (CH, C-3), 67.8 (CH, C$_{cluster}$), 62.3 (CH, C$_{cluster}$) ppm. IR (ATR, cm^{-1}): 3385 (m, νNH), 3240 (s, νOH), 3064 (m-w, νCH), 2592 (s, νBH), 1591–1434 (m-w, νCC), 1519 (s, νNO$_2$), 1266 (m, νCN), 746 (m, νBB); HR-ESI-MS (positive mode, MeCN), m/z [M+H]$^+$: calculated for C$_8$H$_{17}$B$_{10}$N$_2$O$_3$: 297.2243, found 297.2250; the observed isotopic pattern is in agreement with the calculated one. HPLC: t_R = 5.26 min; purity: 99.4% relative area.

1-[N-(1,7-Dicarba-closo-dodecaboran-9-yl)]-2-[O-(1,7-dicarba-closo-dodecaboran-9-yl)]-4-nitrobenzene (5)

5 was synthesized from **3a** (223 mg, 1 mmol), 1 equiv. of 2-amino-5-nitrophenol (154.1 mg, 1 mmol), 3 equiv. of KOt-Bu (336.6 mg, 3 mmol), SPhos-Pd-G4 (39.7 mg, 5 mol%), and SPhos (20.5 mg, 5 mol%) in dry 1,4-dioxane (10 mL). The mixture was stirred at 70 °C for 25 min. Purification via column chromatography with (silica gel, n-hexane/ethyl acetate, 4:1 (v/v)) afforded **5** as a yellow powder. Yield: 36.1% (79.2 mg, 0.18 mmol). Single crystals were obtained by layering a saturated CH$_2$Cl$_2$ solution of **5** with n-hexane. M.p. 184–185 °C. TLC (n-hexane/ethyl acetate, 4:1 (v/v)): R$_f$ = 0.26; ^{1}H-NMR ((CD$_3$)$_2$CO): δ 7.90 (dd, $^3J_{HH}$ = 9.1, 2.6 Hz, 1H, CH$_{aryl}$), 7.83 (d, $^3J_{HH}$ = 2.6 Hz, 1H, CH$_{aryl}$), 7.28 (d, $^3J_{HH}$ = 9.1 Hz, 1H, CH$_{aryl}$), 5.11 (s, 1H, NH), 3.73 (s, 2H, CH$_{cluster}$), 3.64 (s, 2H, CH$_{cluster}$), 3.11–1.53 (br, 9H, BH) ppm. ^{11}B{^{1}H}-NMR ((CD$_3$)$_2$CO): δ 8.3 (s, 1B, BO), 1.3 (s, 1B, BNH), –7.8 (s, 2B, BH), –8.3 (s, 2B, BH), –11.4 (s, 1B, BH), –12.2 (s, 1B, BH), –14.1 (s, 2B, BH), –14.8 (s, 2B, BH), –15.3 (s, 2B, BH), –16.3 (s, 2B, BH), –18.6 (s, 1B, BH), –19.7 (s, 1B, BH), –22.5 (s, 1B, BH), –25.1 (s, 1B, BH) ppm. ^{11}B-NMR ((CD$_3$)$_2$CO): δ 8.3 (s, 1B, BO), 1.3 (s, 1B, BNH), –6.9 to –8.9 (br, 4B, BH), –10.7 to –20.4 (br, 12B, BH), –22.5 (d, J_{BH} = 183.4 Hz, 1B, BH), –25.0 (d, J_{BH} = 185.0 Hz, 1B, BH) ppm. ^{13}C{^{1}H}-NMR ((CD$_3$)$_2$CO): δ 147.8 (C, C-2), 145.2 (C, C-4), 136.8 (C, C-1), 120.3 (CH, C-6), 114.6 (CH, C-5), 110.9 (CH, C-3), 52.5 (CH, C$_{cluster}$), 51.3 (CH, C$_{cluster}$) ppm. IR (ATR, cm^{-1}): 3391 (m, νNH), 3065 (m-w, νCH), 2597 (s, νBH), 1585–1443 (m-w, νCC), 1519 (s, νNO$_2$), 1290 (m, νCN), 730 (m, νBB); HR-ESI-MS (positive mode, MeCN), m/z [M+H]$^+$: calculated for C$_{10}$H$_{27}$B$_{20}$N$_2$O$_3$: 439.4028, found 439.4030; the observed isotopic pattern is in agreement with the calculated one. HPLC: t_R = 7.23 min; purity: 98.3% relative area (254 nm).

Mesylation of the Carboranyl-amino-nitrophenols (2b–4b): The general procedure for mesylation of carborane-NH-nitrophenols was very similar for the three isomers.

A 10 mL round-bottom flask was charged with the corresponding carborane-amino-nitrophenol (**2b–4b**) and 1–5.5 mL of pyridine. The resulting mixture was stirred at –20 °C for 10–15 min. Subsequently, 1.1 equiv. of MsCl (methanesulfonyl chloride) was added dropwise and the reaction mixture was stirred at room temperature until consumption of the starting material was observed by TLC (silica plates, n-hexane/ethyl acetate, 8:2 (v/v)). Then, ice-cold water was added, resulting in a turbid solution. The solution was extracted three times with diethyl ether and the extract was further washed with water (10 mL) and 1 M aqueous HCl (10 mL). The organic phase was dried over MgSO$_4$. Evaporation of the solvent yielded the pure product as light yellow powder.

5-Nitro-2-[N-(1,2-dicarba-closo-dodecaboran-9-yl)]phenyl methanesulfonate (2c)

2c was synthesized from **2b** (1.13 mmol, 335.3 mg), 5.5 mL pyridine, 1.1 equiv. MsCl (1.24 mmol, 96.3 μL), stirring for 3.5 h at room temperature. The addition of 80 mL of ice-cold water gave the product as precipitate, which was isolated via vacuum filtration. Further washing with water and HCl aq. (1 M) yielded the pure product (**2c**) as yellow powder. Yield 52.3% (205.2 mg, 0.548 mmol). Single crystals were obtained by layering the saturated THF solution of **2c** with n-pentane. M.p. = 207–208 °C, TLC (diethyl ether): R$_f$ = 0.48; ^{1}H-NMR ((CD$_3$)$_2$CO): δ 8.11 (d, $^3J_{HH}$ = 2.7 Hz, 1H, CH$_{aryl}$), 8.07 (dd, $^3J_{HH}$ = 9.2, 2.7 Hz, 1H, CH$_{aryl}$), 7.39 (d, $^3J_{HH}$ = 9.2 Hz, 1H, CH$_{aryl}$), 5.42 (s, 1H, NH), 4.61 (s, 2H, CH$_{cluster}$), 3.46 (s, 3H, CH$_3$), 2.99–1.50 (br, 9H, BH) ppm. ^{11}B{^{1}H}-NMR ((CD$_3$)$_2$CO): δ 6.8 (s, 1B, BNH), –4.2 (s, 1B, BH), –10.1 (s, 2B, BH), –14.5 (s, 1B, BH), –15.6 (s, 3B, BH), –16.2 (s, 2B, BH) ppm. ^{11}B-NMR ((CD$_3$)$_2$CO): δ 6.8 (s, 1B, BNH), –4.2 (d, J_{BH} = 148.1 Hz, 1B, BH), –10.1 (d, J_{BH} = 149.6 Hz, 2B,

BH), –13.9 to –16.9 (br, 6B, BH) ppm. ^{13}C{^{1}H}-NMR ((CD$_3$)$_2$CO): δ 147.8 (C, C-1), 136.7 (C, C-5), 135.6 (C, C-2), 123.9 (CH, C-3), 119.1 (CH, C-4), 113.3 (CH, C-6), 52.6 (CH, C$_{cluster}$), 46.1 (CH, C$_{cluster}$), 37.6 (CH, CH$_3$) ppm. IR (ATR, cm^{-1}): 3358 (m, νNH), 3065 (m-w, νCH), 2567 (s, νBH), 1595–1496 (m-w, νCC), 1525 (s, νNO$_2$), 1322 (m, νCN), 1150 (m, νSO), 745 (m, νBB); HR-ESI-MS (positive mode, MeCN), m/z [M+Na]$^+$: calculated for C$_9$H$_{18}$B$_{10}$N$_2$O$_5$SNa: 397.1785, found 397.1840; the observed isotopic pattern is in agreement with the calculated one. HPLC: t_R = 5.83 min; purity: 95.7% relative area.

5-Nitro-2-[N-(1,7-dicarba-closo-dodecaboran-9-yl)]phenyl methanesulfonate (3c)

3c was synthesized from **3b** (0.21 mmol, 62 mg), 1 mL of pyridine, 1.1 equiv. MsCl (0.23 mmol, 17.9 μL), stirring for 21 h at room temperature. The addition of 6 mL of ice-cold water gave the product as precipitate which was isolated via vacuum filtration. Further washing with water and HCl aq (1 M) yielded the pure product (**3c**) as yellow precipitate. Yield 95.2% (74.8 mg, 0.199 mmol). Single crystals were obtained by layering the saturated CH$_2$Cl$_2$ solution of **3c** with n-hexane. M.p. = 120–121 °C, TLC (n-hexane/ethyl acetate, 3:2 (v/v)): R$_f$ = 0.45; ^{1}H-NMR ((CD$_3$)$_2$CO): δ 8.17–8.08 (m, 2H, CH$_{aryl}$), 7.50 (d, $^3J_{HH}$ = 9.2 Hz, 1H, CH$_{aryl}$), 5.64 (s, 1H, NH), 3.74 (s, 2H, CH$_{cluster}$), 3.49 (s, 3H, CH$_3$), 3.11–1.30 (br, 9H, BH) ppm. ^{11}B{^{1}H}-NMR ((CD$_3$)$_2$CO): δ 1.0 (s, 1B, BNH), –7.6 (s, 2B, BH), –11.4 (s, 1B, BH), –14.9 (s, 2B, BH), –15.2 (s, 2B, BH), –18.6 (s, 1B, BH), –22.2 (s, 1B, BH) ppm. ^{11}B-NMR ((CD$_3$)$_2$CO): δ 1.0 (s, 1B, BNH), –7.6 (d, J_{BH} = 162.4 Hz, 2B, BH), –11.4 (d, J_{BH} = 149.0 Hz, 1B, BH), –13.2 to –15.9 (br, 4B, BH), –18.6 (d, J_{BH} = 182.8 Hz, 1B, BH), –22.2 (d, J_{BH} = 183.5 Hz, 1B, BH) ppm. ^{13}C{^{1}H}-NMR ((CD$_3$)$_2$CO): δ 148.0 (C, C-1), 136.9 (C, C-5), 135.8 (C, C-2), 123.9 (CH, C-6), 119.1 (CH, C-4), 113.5 (CH, C-6), 52.7 (CH, C$_{cluster}$), 37.6 (C, CH$_3$) ppm. IR (ATR, cm^{-1}): 3364 (m, νNH), 3066 (m-w, νCH), 2602 (s, νBH), 1591–1440 (m-w, νCC), 1591 (s, νNO$_2$), 1288 (m, νCN), 1153 (m, νSO), 744 (m, νBB); HR-ESI-MS (positive mode, MeCN), m/z [M+H]$^+$: calculated for C$_9$H$_{19}$B$_{10}$N$_2$O$_5$S: 375.2043, found 375.2010; the observed isotopic pattern is in agreement with the calculated one. HPLC: t_R = 5.93 min; purity: 98.9% relative area.

5-Nitro-2-[N-(1,12-dicarba-closo-dodecaboran-2-yl)]phenyl methanesulfonate (4c)

4c was synthesized from **4b** (0.21 mmol, 62 mg), 1 mL of pyridine, 1.1 equiv. MsCl (0.23 mmol, 17.9 μL) after 21 h at room temperature. The addition of 6 mL of ice-cold water resulted in an orange suspension and the product was extracted with diethyl ether (3 × 5 mL). Residual pyridine was removed from the extract by washing with 1 M aqueous HCl (10 mL). Evaporation of the solvent gave the pure product (**4c**) as light-yellow powder. Yield: 99.2% (78 mg, 0.208 mmol). Single crystals were grown by layering the saturated THF solution of **4c** with n-pentane. M.p. = 103–105 °C, TLC (n-hexane/ethyl acetate, 3:2 (v/v)): R$_f$ = 0.67; ^{1}H-NMR ((CD$_3$)$_2$CO): δ 8.20 (dd, $^3J_{HH}$ = 9.0, 2.7 Hz, 1H, CH$_{aryl}$), 8.18 (d, $^3J_{HH}$ = 2.6 Hz, 1H, CH$_{aryl}$), 7.74 (d, $^3J_{HH}$ = 9.0 Hz, 1H, NH), 3.86 (s, 1H, CH$_{cluster}$), 3.57 (s, 1H, CH$_{cluster}$), 3.46 (s, 3H, CH$_3$), 3.05–1.56 (br, 9H, BH) ppm. ^{11}B{^{1}H}-NMR ((CD$_3$)$_2$CO): δ –3.9 (s, 1B, BNH), –14.2 (s, 2B, BH), –15.7 (s, 3B, BH), –16.6 (s, 3B, BH), –20.2 (s, 1B, BH) ppm. ^{11}B-NMR ((CD$_3$)$_2$CO): δ –3.9 (s, 1B, BNH), –13.5 to –17.3 (br, 8B, BH), –20.2 (d, J_{BH} = 169.1 Hz, 1B, BH) ppm. ^{13}C{^{1}H}-NMR ((CD$_3$)$_2$CO): δ 147.2 (C, C-1), 138.0 (C, C-5), 136.2 (C, C-2), 123.9 (CH, C-3), 119.1 (CH, C-4), 114.6 (CH, C-6), 67.4 (CH, C$_{cluster}$), 62.5 (CH, C$_{cluster}$), 37.4 (C, CH$_3$) ppm. IR (ATR, cm^{-1}): 3355 (m, νNH), 3060 (m-w, νCH), 2609 (s, νBH), 1591–1458 (m-w, νCC), 1591 (s, νNO$_2$), 1291 (m, νCN), 1151 (m, νSO), 740 (m, νBB); HR-ESI-MS (positive mode, MeCN), m/z [M+H]$^+$: calculated for C$_9$H$_{19}$B$_{10}$N$_2$O$_5$S: 375.2043, found 375.2030; the observed isotopic pattern is in agreement with the calculated one. HPLC: t_R = 6.33 min; purity: 98.8% relative area.

Deboronation of 2c: Sodium rac-2-[N-(7,8-dicarba-nido-undecahydroborat-6-yl)-5-nitrophenyl] methanesulfonate (6)

In a 100 mL round-bottom Schlenk flask, a 10 mL mixture of ethanol/water (3:2, v/v) was degassed for 30 min under nitrogen flow. Then, **2c** (100 mg, 0.27 mmol) and 5 equiv. NaF (56.7 mg, 1.35 mmol) were added and the mixture was stirred at 90 °C for 3 h. Then, the reaction mixture was cooled to room temperature and it was concentrated under reduced pressure. The desired product (**6**) was suspended with 100 mL

ice cold water. The product was extracted with ethyl acetate (3 × 100 mL), and dried over MgSO$_4$. Evaporation of the solvent gave the crude product as orange-red paste. Further purification via column chromatography (silica gel, n-hexane/ethyl acetate, 3:2–1:1 (v/v)) yielded the pure product as red-orange powder. Yield 96.3% (100.2 mg, 0.26 mmol). M.p. = >310 °C decomposition. TLC (ethyl acetate): R$_f$ = 0.17; ^{1}H-NMR ((CD$_3$)$_2$CO): δ 7.98 (d, $^3J_{HH}$ = 2.6 Hz, 1H, CH_{aryl}), 7.93 (dd, $^3J_{HH}$ = 9.4, 2.7 Hz, 1H, CH_{aryl}), 7.70 (d, $^3J_{HH}$ = 9.5 Hz, 1H, CH_{aryl}), 4.89 (s, 1H, NH), 3.29 (s, 3H, CH_3), 1.89 (s, 1H, C$H_{cluster}$), 1.66 (s, 1H, C$H_{cluster}$), 2.49–0.88 (br, 8H, BH) ppm. ^{11}B{^{1}H}-NMR ((CD$_3$)$_2$CO): δ –0.8 (s, 1B, BNH), –11.2 (s, 1B, BH), –14.1 (s, 1B, BH), –18.8 (s, 1B, BH), –20.9 (s, 1B, BH), –22.5 (s, 1B, BH), –24.4 (s, 1B, BH), –31.3 (s, 1B, BH), –37.5 (s, 1B, BH) ppm. ^{11}B-NMR ((CD$_3$)$_2$CO): δ –0.8 (s, 1B, BNH), –11.2 (d, J_{BH} = 136.0 Hz, 1B, BH), –14.2 (d, J_{BH} = 139.0 Hz, 1B, BH), –18.2 to –25.1 (br, 4B, BH), –31.5 (d, J_{BH} = 141.0 Hz, 1B, BH), –37.5 (d, J_{BH} = 142.4 Hz, 1B, BH) ppm. ^{13}C{^{1}H}-NMR ((CD$_3$)$_2$CO): δ 149.8 (C, C-1), 135.3 (C, C-5), 133.8 (C, C-2), 123.8 (CH, C-6), 118.4 (CH, C-4), 113.8 (CH, C-6), 37.3 (C, CH$_3$), 32.9 (C, C$_{cluster}$) ppm. IR (ATR, cm^{-1}): 3376 (m, νNH), 2922 (m-w, νCH), 2501 (s, νBH), 1593–1482 (m-w, νCC), 1593 (s, νNO$_2$), 1289 (m, νCN), 1150 (m, νSO), 744 (m, νBB); HR-ESI-MS (negative mode, MeCN), m/z [M–Na]$^-$: calculated for C$_9$H$_{18}$B$_9$N$_2$O$_5$S: 364.1810, found 364.1860; the observed isotopic pattern is in agreement with the calculated one. HPLC: t_R = 6.13 min; purity: 98.5% relative area.

Biological Evaluation for COX Inhibition and Cytotoxic Potential: Evaluation for COX Inhibition: The COX inhibition activity against ovine COX-1 and human COX-2 was determined using the fluorescence-based COX assay COX Fluorescent Inhibitor Screening Assay Kit (Cayman Chemical Company, Ann Arbor, MI, USA) according to the manufacturer's instructions as previously reported.[64,65]

Determination of Lipophilicity: The log$D_{7.4, HPLC}$ values (Table S10, Supporting Information) were determined[87] utilizing an HPLC method originally described by Donovan and Pescatore.[76] The following HPLC system was used: Agilent 1100 HPLC (binary pump G1312A, autosampler G1313A, column oven G1316A, degasser G1322A, UV detector 1314A, γ detector Gabi Star (Raytest); column ODP-50 4B (Shodex Asahipak 50 × 4.6 mm); eluent: MeOH/phosphate buffer (10 mM, pH = 7.4), gradient $t_{0\,min}$ 30/70–$t_{25\,min}$ 95/5–$t_{27\,min}$ 95/5–$t_{28\,min}$ 30/70–$t_{40\,min}$ 30/70, flow rate = 0.6 mL min^{-1}. Oxycarboxin (t_R = 9.02 min, log$D_{7.4}$ = 1.13) and triphenylene (t_R = 29.47 min, log$D_{7.4}$ = 5.49) served as references. Toluene served as control and log$D_{7.4}$ was found to be 2.72 (literature log$D_{7.4}$ = 2.72[76]).

Evaluation for Cytotoxic Potential: Reagents and Cells: Roswell Park Memorial Institute 1640 (RPMI 1640) medium, RPMI 1640 medium without Phenol red, Dulbecco's modified Eagle medium (DMEM) high glucose, fetal bovine serum (FBS), and trypsin/ethylenediaminetetraacetic acid (EDTA) were purchased from Capricorn Scientific GmbH (Hessen, Germany). Phosphate-buffered saline (PBS), DMSO, PI, CV, and carboxyfluorescein diacetate succinimidyl ester (CFSE) were bought from Sigma-Aldrich (St. Louis, MO, USA). The penicillin–streptomycin solution was obtained from Biological Industries (Cromwell, CT, USA). Paraformaldehyde (PFA) was acquired from Serva (Heidelberg, Germany). Annexin V (AnnV)-fluorescein isothiocyanate was purchased from BD Pharmingen (San Diego, CA, USA), while ApoStat was from R&D Systems (Minneapolis, MN, USA). DHR and 4-amino-5-methylamino-2′,7′-difluorofluorescein (DAF-FM) diacetate were obtained from Thermo Fisher Scientific (Waltham, MA, USA). MTT was bought from AppliChem (Darmstadt, Germany).

A549, A375, HT29, HCT116, MCF-7, and MRC-5 cell lines were acquired from American Type Culture Collection (ATCC, Rockville, VA, USA).

All listed cell lines were cultivated in 4-(2-hydroxyethyl)-1-piperazineethanesulfonic acid (HEPES)-buffered RPMI-1640 while DMEM was used for A549 cell line. Both media previously were supplemented with 10% heat-inactivated FBS, 2 mM L-glutamine, 0.01% sodium pyruvate, and antibiotics (penicillin 100 units mL^{-1} and streptomycin 100 µg mL^{-1}). All cell lines were grown in T-25 flasks at 37 °C in a humidified atmosphere with 5% CO$_2$. Cells were washed with PBS and detached by using trypsin/EDTA (0.05% in PBS) prior to cell passaging and seeding.

To determine viability, cells were seeded in 96-well plates at different densities: A549 (5 × 10^3 cells per well), A375 (8 × 10^3 cells per well), HT29 (6.5 × 10^3 cells per well), HCT116 (6 × 10^3 cells per well), MCF-7 (7 × 10^3 cells per well), and MRC-5 (5 × 10^3 cells per well). For flow cytometric analyses MCF-7 cells were seeded in 6-well plates at density 2 × 10^5 cells per well.

Peritoneal exudate cells (PEC) were isolated from peritoneal cavity of C57BL/6 mice, by rinsing with ice-cold PBS. C57BL/6 mice originated from animal facility at the Institute for Biological Research "Siniša Stanković" (IBISS), National Institute of the Republic of Serbia, University of Belgrade (Belgrade, Serbia). After isolation, peritoneal exudate cells were cultivated in HEPES-buffered RPMI-1640 medium supplemented with 5% heat inactivated FBS, 2 mM L-glutamine, 0.01% sodium pyruvate, and antibiotics, at 37 °C in a humidified environment with 5% CO$_2$. Subsequently, cells were seeded at density 1.5 × 10^5 cells per well in 96-well plates and allowed to adhere for 2 h. Before treatment, nonadherent cells were removed. Post 72 h of the treatment, cell viability was determined using CV assay. The manipulation of animals was in accordance with the rules of the European Union and approved by the local Institutional Animal Care and Use Committee and the European Community guidelines (EEC Directive of 1986; 86/609/EEC). Experimental protocols were approved and granted by the national licensing committee at the Department of Animal Welfare, Veterinary Directorate, Ministry of Agriculture, Forestry and Water Management of the Republic of Serbia (Permission No. 323-07-02147/2023-05).

The stocks were prepared in DMSO at a concentration of 200 mM and stored at –20 °C before the usage. The final concentration of DMSO in working solutions was 0.2%.

Colorimetric Assays for Cellular Viability: Cells were seeded overnight and treated with **Ref-1**, **1**, **2b–4b**, **2c–4c**, **5**, and **6** for 72 h over a wide range of concentrations. Thereafter, the supernatant was discarded and the cells were washed with PBS. Finally, the cells were incubated with MTT solution (0.5 mg mL^{-1}) at 37 °C and purple-brown formazan crystals were formed. Afterwards, the dye was removed and DMSO was added in order to dissolve the formed formazan crystals.

For CV assay, treated cells were fixed with 4% PFA for 10 min. After that, cells were stained with 1% CV solution for 15 min at room temperature (RT), washed with PBS, and the dye was dissolved in 33% acetic acid.

For both assays, absorbance was measured at λ_{max} = 540 nm, with the reference λ_{max} = 670 nm. Cell viability was calculated as a percentage of control (100%). All experiments were repeated three times.

Apoptosis, Caspase Activation: Cells were exposed to IC$_{50}$ values of the selected compounds **4b** (10 µM), **4c** (12 µM), and **1** (70 µM) for 72 h.

For the detection of apoptosis, cells were stained with AnnV according to the manufacturer guidelines and PI (15 µg mL^{-1}) for 15 min at RT protected from light. Finally, cells were resuspended in AnnV-binding buffer and analyzed by flow cytometry. Thereafter, to ascertain whether apoptosis was mediated by activation of caspases, cells were incubated with pan-caspase inhibitor ApoStat for 30 min at 37 °C. At the end, cells were washed with PBS and analyzed. For both methods, a CytoFLEX Flow Cytometer (Beckman Coulter, Brea, CA, USA) and the CytExpert software were used to determine fluorescence intensity.

Detection of Cell Proliferation: The effect of compounds **1**, **4b**, and **4c** on the proliferation rate was analyzed by CFSE staining. Cells were prestained with CFSE (1 µM) for 10 min at 37 °C. Afterward, cells were washed, seeded, and treated with IC$_{50}$ doses of **1**, **4b**, and **4c** for 72 h. Lastly, cells were trypsinized, resuspended in PBS, and analyzed using a CytoFLEX Flow Cytometer.

Measurement of Generation of ROS/RNS: The production of ROS/RNS was detected by prestaining the cells with DHR (1 µM) for 20 min at 37 °C and followed by treatment with IC$_{50}$ doses of **1**, **4b**, and **4c** for 48 h. Then, cells were washed, trypsinized, and analyzed by flow cytometry. Additionally, after cells were treated with IC$_{50}$ doses of **1**, **4b**, and **4c** for 48 h, nitric oxide was quantified with DAF-FM staining (5 µM) for 60 min at 37 °C in the phenol red-free medium. Finally, cells were washed, trypsinized, resuspended in PBS, and analyzed using flow cytometry. For both methods, a CytoFLEX Flow Cytometer was used.

PI Staining on Chamber Slides: MCF-7 cells were seeded overnight at a density of 3.5 × 10^4 followed by treatment with IC$_{50}$ doses of **1**, **4b**, and **4c**

for 72 h. Subsequently, cells were washed with PBS, fixed with 4% PFA for 15 min at RT, and stained with a solution of PI in a concentration of 50 µg mL^{-1} with EDTA pH 8.0 (0.1 mM), Triton X-100 (0.1%), and RNase (85 µg mL^{-1}) in PBS for 1.5 min. At the end, mounting medium (Fluoromount G, Thermo Fisher Scientific, Waltham, MA, USA) was used for covering the slides, and the slides were analyzed with a Zeiss AxioObserver Z1 inverted fluorescence microscope (Carl Zeiss AG, Oberkochen, Germany) at 200× enlargement.

Statistical Analysis: The data shown represent the means ± standard deviation (SD) of three independent experiments. Student's *t*-test was used to assess the significance between samples, and two-sided *p*-values of less than 0.05 were considered statistically significant.

Supporting Information

Supporting Information is available from the Wiley Online Library or from the author.

Conflict of Interest

The authors declare no conflict of interest.

Data Availability Statement

The data that support the findings of this study are available in the Supporting Information of this article.

[1] A. Bennett, G. Villa, *Expert Opin. Pharmacother.* **2000**, *1*, 277.

[2] A. K. Singla, M. Chawla, A. Singh, *J. Pharm. Pharmacol.* **2000**, *52*, 467.

[3] F. Toscani, M. Gallucci, I. Scaricabarozzi, *Drugs* **1993**, *46*, 156.

[4] a) A. Binning, *Clin. J. Pain* **2007**, *23*, 565; b) M. Bianchi, *Future Rheumatol.* **2006**, *1*, 533.

[5] H. Suleyman, E. Cadirci, A. Albayrak, Z. Halici, *Curr. Med. Chem.* **2008**, *15*, 278.

[6] K. D. Rainsford, *Inflammopharmacology* **2006**, *14*, 120.

[7] G. E. Senna, G. Passalacqua, G. Andri, A. R. Dama, M. Albano, L. Fregonese, L. Andri, *Drug Saf.* **1996**, *14*, 94.

[8] M. Catarro, J. L. Serrano, S. S. Ramos, S. Silvestre, P. Almeida, *Bioorg. Chem.* **2019**, *88*, 102966.

[9] T. Jia-Jun, L. Su-Mei, Y. Liang, M. Ju-Ke, M. Ya-Kui, W. Hai-Bo, X. Wei, *Head Neck Oncol.* **2012**, *4*, 7.

[10] A. Bernareggi, *Clin. Pharmacokinet.* **1998**, *35*, 247.

[11] R. G. Ferreira, L. E. M. Narvaez, K. M. M. Espíndola, A. C. R. S. Rosario, W. G. N. Lima, M. C. Monteiro, *Front. Oncol.* **2021**, *11*, 594917.

[12] M. Sofia, A. Molino, M. Mormile, A. Stanziola, I. Scaricabarozzi, L. Carratù, *Drugs* **1993**, *46*, 111.

[13] A. Ward, R. N. Brogden, *Drugs* **1988**, *36*, 732.

[14] a) M. F. P. Werner, G. E. P. Souza, A. R. Zampronio, *Eur. J. Pharmacol.* **2006**, *543*, 181; b) A. Bernareggi, *Drugs* **1993**, *46*, 64.

[15] J. Kwon, S. Kim, H. Yoo, E. Lee, *PLoS One* **2019**, *14*, 0209264.

[16] M. Donati, A. Conforti, M. C. Lenti, A. Capuano, O. Bortolami, D. Motola, U. Moretti, A. Vannacci, C. Rafaniello, A. Vaccheri, E. Arzenton, R. Bonaiuti, L. Sportiello, R. Leone, *Br. J. Clin. Pharmacol.* **2016**, *82*, 238.

[17] a) W. Sbeit, N. Krivoy, M. Shiller, R. Farah, H. I. Cohen, L. Struminger, R. Reshef, *Ann. Pharmacother.* **2001**, *35*, 1049; b) F. Bessone, L. Colombato, E. Fassio, M. V. Reggiardo, J. Vorobioff, H. Tanno, *Anti-Inflamm. Anti-Allergy Agents Med. Chem.* **2010**, *9*, 355.

[18] B. N. Sağlık, D. Osmaniye, S. Levent, U. A. Çevik, B. K. Çavuşoğlu, Y. Özkay, Z. A. Kaplancıklı, *Eur. J. Med. Chem.* **2021**, *209*, 112918.

[19] T. Güngör, A. Ozleyen, Y. B. Yılmaz, P. Siyah, M. Ay, S. Durdağı, T. B. Tumer, *Eur. J. Med. Chem.* **2021**, *221*, 113566.

[20] Y. Yamamoto, T. Hisa, J. Arai, Y. Saito, F. Yamamoto, T. Mukai, T. Ohshima, M. Maeda, Y. Ohkubo, *Bioorg. Med. Chem.* **2015**, *23*, 6807.

[21] a) B. S. Selinsky, K. Gupta, C. T. Sharkey, P. J. Loll, *Biochemistry* **2001**, *40*, 5172; b) B. J. Orlando, M. G. Malkowski, *J. Biol. Chem.* **2016**, *291*, 15069; c) S. L. Curry, S. M. Cogar, J. L. Cook, *J. Am. Anim. Hosp. Assoc.* **2005**, *41*, 298.

[22] K. D. Rainsford, *Nimesulide: Actions and Uses* (Ed: K. D. Rainsford), Birkhauser, Basel **2005**.

[23] N. Osafo, C. Agyare, D. D. Obiri, A. O. Antwi, in *Nonsteroidal Anti-Inflammatory Drugs* (Ed: A. G. A. Al-kaf), InTech, Rijeka, Croatia **2017**.

[24] a) T. Miyamoto, N. Ogino, S. Yamamoto, O. Hayaishi, *J. Biol. Chem.* **1976**, *251*, 2629; b) W. L. Xie, J. G. Chipman, D. L. Robertson, R. L. Erikson, D. L. Simmons, *Proc. Nat. Acad. Sci. USA* **1991**, *88*, 2692; c) D. A. Kujubu, B. S. Fletcher, B. C. Varnum, R. W. Lim, H. R. Herschman, *J. Biol. Chem.* **1991**, *266*, 12866; d) R. M. Garavito, A. M. Mulichak, *Annu. Rev. Biophys. Biomol. Struct.* **2003**, *32*, 183.

[25] M. Hamberg, B. Samuelsson, *J. Biol. Chem.* **1967**, *242*, 5344.

[26] a) D. E. Griswold, J. L. Adams, *Med. Res. Rev.* **1996**, *16*, 181; b) R. Garavito, D. L. DeWitt, *Biochim. Biophys. Acta, Mol. Cell Biol. Lipids* **1999**, *1441*, 278.

[27] P. K. Deb, R. P. Mailabaram, B. Al-Jaidi, M. J. Saadh, in *Nonsteroidal Anti-Inflammatory Drugs* (Ed: A. G. A. Al-kaf), InTech, Rijeka, Croatia **2017**.

[28] P. Stockmann, M. Gozzi, R. Kuhnert, M. B. Sárosi, E. Hey-Hawkins, *Chem. Soc. Rev.* **2019**, *48*, 3497.

[29] a) J. Vane, J. Botting, R. Botting, *Improved Non-Steroid Anti-Inflammatory Drugs: COX-2 Enzyme Inhibitors*, Springer, Dordrecht, Netherlands **1996**; b) R. M. Botting, *Pharmacol. Rep.* **2010**, *62*, 518.

[30] T. Grosser, S. Fries, G. A. FitzGerald, *J. Clin. Invest.* **2006**, *116*, 4.

[31] M. M. Wolfe, D. R. Lichtenstein, G. Singh, *N. Engl. J. Med.* **1999**, *340*, 1888.

[32] a) L. J. Marnett, *Annu. Rev. Pharmacol. Toxicol.* **2009**, *49*, 265; b) N.-A. Mohsin, M. Irfan, *Med. Chem. Res.* **2020**, *29*, 809; c) A. Zarghi, S. Arfaei, *Iran. J. Pharm. Res.* **2011**, *10*, 655.

[33] a) A. L. Blobaum, L. J. Marnett, *J. Med. Chem.* **2007**, *50*, 1425; b) V. Limongelli, M. Bonomi, L. Marinelli, F. L. Gervasio, A. Cavalli, E. Novellino, M. Parrinello, *Proc. Nat. Acad. Sci. USA* **2010**, *107*, 5411; c) L. J. Mengle-Gaw, B. D. Schwartz, *Mediators Inflammation* **2002**, *11*, 275.

[34] C. Michaux, C. Charlier, *Mini-Rev. Med. Chem.* **2004**, *4*, 603.

[35] J. A. Cairns, *Can. J. Cardiol.* **2007**, *23*, 125.

[36] a) M. Barbarić, M. Kralj, M. Marjanović, I. Husnjak, K. Pavelić, J. Filipović-Grcić, D. Zorc, B. Zorc, *Eur. J. Med. Chem.* **2007**, *42*, 20; b) B. Mathew, J. V. Hobrath, W. Lu, Y. Li, R. C. Reynolds, *Med. Chem. Res.* **2017**, *26*, 3038.

[37] a) M. J. Thun, S. J. Henley, C. Patrono, *J. Natl. Cancer Inst.* **2002**, *94*, 252; b) C. Rüegg, R. Zaric, R. Stupp, *Ann. Med.* **2003**, *35*, 476; c) S. Zappavigna, A. M. Cossu, A. Grimaldi, M. Bocchetti, G. A. Ferraro, G. F. Nicoletti, R. Filosa, M. Caraglia, *Int. J. Mol. Sci.* **2020**, *21*, 2605.

[38] a) R. S. Y. Wong, *Adv. Pharmacol. Sci.* **2019**, *2019*, 3418975; b) R. Kumar, *J. Nanomed. Nanotechnol.* **2016**, *7*, e140.

[39] A. Kazberuk, I. Zareba, J. Palka, A. Surazynski, *Pharmacol. Rep.* **2020**, *72*, 1152.

[40] a) G. Landskron, M. de La Fuente, P. Thuwajit, C. Thuwajit, M. A. Hermoso, *J. Immunol. Res.* **2014**, *2014*, 149185; b) O. C. Trifan, T. Hla, *J. Cell. Mol. Med.* **2003**, *7*, 207.

[41] a) J. L. Liggett, X. Zhang, T. E. Eling, S. J. Baek, *Cancer Lett.* **2014**, *346*, 217; b) E. Gurpinar, W. E. Grizzle, G. A. Piazza, *Front. Oncol.* **2013**, *3*, 181; c) E. Gurpinar, W. E. Grizzle, G. A. Piazza, *Clin. Cancer Res.* **2014**, *20*, 1104.

[42] W. Li, H. Zhang, R. Xu, G. Zhuo, Y. Hu, J. Li, *Med. Oncol.* **2008**, *25*, 172.

[43] C. T. Sengel-Turk, C. Hascicek, F. Bakar, E. Simsek, *AAPS PharmSciTech* **2017**, *18*, 393.

[44] J. F. Valliant, K. J. Guenther, A. S. King, P. Morel, P. Schaffer, O. O. Sogbein, K. A. Stephenson, *Coord. Chem. Rev.* **2002**, *232*, 173.

[45] a) M. Scholz, A. L. Blobaum, L. J. Marnett, E. Hey-Hawkins, *Bioorg. Med. Chem.* **2011**, *19*, 3242; b) M. Scholz, G. N. Kaluđerović, H. Kommera, R. Paschke, J. Will, W. S. Sheldrick, E. Hey-Hawkins, *Eur. J. Med. Chem.* **2011**, *46*, 1131; c) B. Schwarze, M. Gozzi, C. Zilberfain, J. Rüdiger, C. Birkemeyer, I. Estrela-Lopis, E. Hey-Hawkins, *J. Nanopart. Res.* **2020**, *22*, 1533.

[46] Y. Chen, F. Du, L. Tang, J. Xu, Y. Zhao, X. Wu, M. Li, J. Shen, Q. Wen, C. H. Cho, Z. Xiao, *Mol. Ther. Oncol.* **2022**, *24*, 400.

[47] S. Paskaš, B. Murganić, R. Kuhnert, E. Hey-Hawkins, S. Mijatović, D. Maksimović-Ivanić, *Molecules* **2022**, *27*, 4503.

[48] R. N. Grimes, in *Carboranes*, Elsevier, Amsterdam **2016**, pp. 945–984.

[49] E. Hey-Hawkins, C. V. Teixidor, *Boron-Based Compounds: Potential and Emerging Applications in Medicine*, Oxford University Press, Oxford, UK **2018**.

[50] M. Scholz, E. Hey-Hawkins, *Chem. Rev.* **2011**, *111*, 7035.

[51] S. Braun, S. Paskas, M. Laube, S. George, B. Hofmann, P. Lönnecke, D. Steinhilber, J. Pietzsch, S. S. Mijatović, D. Maksimović-Ivanić, E. Hey-Hawkins, *Adv. Ther.* **2023**, *6*, 2200252.

[52] R. N. Grimes, in *Carboranes*, Elsevier, Amsterdam **2016**, pp. 283–502.

[53] R. N. Grimes, in *Carboranes*, Elsevier, Amsterdam **2016**, pp. 7–18.

[54] J. F. Sieckhaus, N. S. Semenuk, T. A. Knowles, H. Schroeder, *Inorg. Chem.* **1969**, *8*, 2452.

[55] a) E. O.-Z. Mason, C. A. Mason, M. W. Lee Jr, *Med. Chem.* **2019**, *9*, 44; b) D. J. Worm, P. Hoppenz, S. Els-Heindl, M. Kellert, R. Kuhnert, S. Saretz, J. Köbberling, B. Riedl, E. Hey-Hawkins, A. G. Beck-Sickinger, *J. Med. Chem.* **2020**, *63*, 2358; c) Y. Sevryugina, R. L. Julius, M. F. Hawthorne, *Inorg. Chem.* **2010**, *49*, 10627; d) R. Kuhnert, M.-B. Sárosi, S. George, P. Lönnecke, B. Hofmann, D. Steinhilber, S. Steinmann, R. Schneider-Stock, B. Murganić, S. Mijatović, D.

Maksimović-Ivanić, E. Hey-Hawkins, *ChemMedChem* **2019**, *14*, 255; e) M. Kellert, D. J. Worm, P. Hoppenz, M. B. Sárosi, P. Lönnecke, B. Riedl, J. Koebberling, A. G. Beck-Sickinger, E. Hey-Hawkins, *Dalton Trans.* **2019**, *48*, 10834; f) D. A. Gruzdev, G. L. Levit, V. P. Krasnov, V. N. Charushin, *Coord. Chem. Rev.* **2021**, *433*, 213753; g) A. F. Armstrong, J. F. Valliant, *Dalton Trans.* **2007**, 4240.

[56] R. Kuhnert, L. Kuhnert, M.-B. Sárosi, S. George, D. Draca, S. Paskas, B. Hofmann, D. Steinhilber, W. Honscha, S. Mijatović, D. Maksimović-Ivanić, E. Hey-Hawkins, *ChemMedChem* **2022**, *17*, 202100588.

[57] F. Issa, M. Kassiou, L. M. Rendina, *Chem. Rev.* **2011**, *111*, 5701.

[58] A. Marfavi, P. Kavianpour, L. M. Rendina, *Nat. Rev. Chem.* **2022**, *6*, 486.

[59] B. C. Das, N. K. Nandwana, S. Das, V. Nandwana, M. A. Shareef, Y. Das, M. Saito, L. M. Weiss, F. Almaguel, N. S. Hosmane, T. Evans, *Molecules* **2022**, *27*, 2615.

[60] K. Messner, B. Vuong, G. K. Tranmer, *Pharmaceuticals* **2022**, *15*, 264.

[61] a) M. Laube, W. Neumann, M. Scholz, P. Lönnecke, B. Crews, L. J. Marnett, J. Pietzsch, T. Kniess, E. Hey-Hawkins, *ChemMedChem* **2013**, *8*, 329; b) S. Saretz, G. Basset, L. Useini, M. Laube, J. Pietzsch, D. Drača, D. Maksimović-Ivanić, J. Trambauer, H. Steiner, E. Hey-Hawkins, *Molecules* **2021**, *26*, 2843; c) M. Scholz, M. Steinhagen, J. T. Heiker, A. G. Beck-Sickinger, E. Hey-Hawkins, *ChemMedChem* **2011**, *6*, 89; d) A. Buzharevski, S. Paskas, M. Laube, P. Lönnecke, W. Neumann, B. Murganić, S. Mijatović, D. Maksimović-Ivanić, J. Pietzsch, E. Hey-Hawkins, *ACS Omega* **2019**, *4*, 8824; e) A. Buzharevski, S. Paskas, M.-B. Sárosi, M. Laube, P. Lönnecke, W. Neumann, D. Maksimović-Ivanić, J. Pietzsch, E. Hey-Hawkins, *ChemMedChem* **2019**, *14*, 315; f) A. Buzharevski, S. Paskaš, M.-B. Sárosi, M. Laube, P. Lönnecke, W. Neumann, B. Murganić, S. Mijatović, D. Maksimović-Ivanić, J. Pietzsch, E. Hey-Hawkins, *Sci. Rep.* **2020**, *10*, 4827.

[62] M. Scholz, K. Bensdorf, R. Gust, E. Hey-Hawkins, *ChemMedChem* **2009**, *4*, 746.

[63] M. Scholz, A. L. Blobaum, L. J. Marnett, E. Hey-Hawkins, *Bioorg. Med. Chem.* **2012**, *20*, 4830.

[64] L. Useini, M. Mojić, M. Laube, P. Lönnecke, J. Dahme, M. B. Sárosi, S. Mijatović, D. Maksimović-Ivanić, J. Pietzsch, E. Hey-Hawkins, *ACS Omega* **2022**, *7*, 24282.

[65] L. Useini, M. Mojić, M. Laube, P. Lönnecke, S. Mijatović, D. Maksimović-Ivanić, J. Pietzsch, E. Hey-Hawkins, *ChemMedChem* **2023**, *18*, 202200583.

[66] D. J. Abraham, A. Burger, *Burger's Medicinal Chemistry and Drug Discovery: Autocoids, Diagnostics and Drugs for New Biology*, Vol. 4, Wiley, Hoboken, NJ **2003**.

[67] B. Su, E. S. Diaz-Cruz, S. Landini, R. W. Brueggemeier, *J. Med. Chem.* **2006**, *49*, 1413.

[68] K. Nakamura, K. Tsuji, N. Konishi, H. Okumura, M. Matsuo, *Chem. Pharmaceut. Bull.* **1993**, *41*, 894.

[69] a) F. Julémont, X. de Leval, C. Michaux, J. Damas, C. Charlier, F. Durant, B. Pirotte, J.-M. Dogné, *J. Med. Chem.* **2002**, *45*, 5182; b) F. Julémont, X. de Leval, C. Michaux, J.-F. Renard, J.-Y. Winum, J.-L. Montero, J. Damas, J.-M. Dogné, B. Pirotte, *J. Med. Chem.* **2004**, *47*, 6749.

[70] R. M. Dziedzic, L. M. A. Saleh, J. C. Axtell, J. L. Martin, S. L. Stevens, A. T. Royappa, A. L. Rheingold, A. M. Spokoyny, *J. Am. Chem. Soc.* **2016**, *138*, 9081.

[71] R. M. Dziedzic, A. M. Spokoyny, *Chem. Commun.* **2019**, *55*, 430.

[72] K. Z. Kabytaev, S. N. Mukhin, I. V. Glukhov, Z. A. Starikova, V. I. Bregadze, I. P. Beletskaya, *Organometallics* **2009**, *28*, 4758.

[73] I. P. Beletskaya, V. I. Bregadze, K. Z. Kabytaev, G. G. Zhigareva, P. V. Petrovskii, I. V. Glukhov, Z. A. Starikova, *Organometallics* **2007**, *26*, 2340.

**ADVANCED
SCIENCE NEWS**

www.advancedsciencenews.com

**ADVANCED
THERAPEUTICS**

www.advtherap.com

[74] S. N. Mukhin, K. Z. Kabytaev, G. G. Zhigareva, I. V. Glukhov, Z. A. Starikova, V. I. Bregadze, I. P. Beletskaya, *Organometallics* **2008**, *27*, 5937.

[75] a) A. Ahmed, I. Shafique, A. Saeed, G. Shabir, A. Saleem, P. Taslimi, T. Taskin Tok, M. Kirici, E. M. Üç, M. Z. Hashmi, *Eur. J. Med. Chem. Rep.* **2022**, *6*, 100082; b) A.-M. Rayar, N. Lagarde, C. Ferroud, J.-F. Zagury, M. Montes, M. Sylla-Iyarreta Veitia, *Curr. Top. Med. Chem.* **2017**, *17*, 2935.

[76] S. F. Donovan, M. C. Pescatore, *J. Chromatogr., A* **2002**, *952*, 47.

[77] a) Y. K. Lee, S. Y. Park, Y. M. Kim, W. S. Lee, O. J. Park, *Exp. Mol. Med.* **2009**, *41*, 201; b) A. M. Tari, A.-M. Simeone, Y.-J. Li, Y. Gutierrez-Puente, S. Lai, W. F. Symmans, *Lab. Invest.* **2005**, *85*, 1357; c) Z.-J. Dai, X.-B. Ma, H.-F. Kang, J. Gao, W.-L. Min, H.-T. Guan, Y. Diao, W.-F. Lu, X.-J. Wang, *Cancer Cell Int.* **2012**, *12*, 53.

[78] T. L. Larkins, M. Nowell, S. Singh, G. L. Sanford, *BMC Cancer* **2006**, *6*, 181.

[79] M. Markelić, D. Drača, T. Krajnović, Z. Jović, M. Vuksanović, D. Koruga, S. Mijatović, D. Maksimović-Ivanić, *Nanomaterials* **2022**, *12*, 1331.

[80] R. K. Harris, E. D. Becker, S. M. Cabral De Menezes, R. Goodfellow, P. Granger, *Concepts Magn. Reson.* **2002**, *14*, 326.

[81] Isotope Distribution Calculator and Mass Spec Plotter, https://www.sisweb.com/mstools/isotope.htm.

[82] CrysAlisPro Software system, Rigaku Corporation, Oxford, UK.

[83] SCALE3 ABSPACK. Empirical Absorption Correction Using Spherical Harmonics, Oxford Diffraction, **2006**.

[84] G. M. Sheldrick, *Acta Crystallogr.* **2015**, *A71*, 3.

[85] G. M. Sheldrick, *Acta Crystallogr.* **2015**, *C71*, 3.

[86] N. C. Bruno, N. Niljianskul, S. L. Buchwald, *J. Org. Chem.* **2014**, *79*, 4161.

[87] R. Wodtke, J. Wodtke, S. Hauser, M. Laube, D. Bauer, R. Rothe, C. Neuber, M. Pietsch, K. Kopka, J. Pietzsch, R. Lösser, *J. Med. Chem.* **2021**, *64*, 3462.